

Automatic phytoplankton image smoothing through integrated dual image histogram specification and enhanced background removal method

Mohd Aiman Syahmi Kamarul Baharin, Ahmad Shahrizan Abdul Ghani, Normawaty Mohammad-Noor, Hasnun Nita Ismail & Syafiq Qhushairy Syamsul Amri

To cite this article: Mohd Aiman Syahmi Kamarul Baharin, Ahmad Shahrizan Abdul Ghani, Normawaty Mohammad-Noor, Hasnun Nita Ismail & Syafiq Qhushairy Syamsul Amri (2022): Automatic phytoplankton image smoothing through integrated dual image histogram specification and enhanced background removal method, The Imaging Science Journal, DOI: [10.1080/13682199.2022.2149067](https://doi.org/10.1080/13682199.2022.2149067)

To link to this article: <https://doi.org/10.1080/13682199.2022.2149067>



Published online: 27 Nov 2022.



Submit your article to this journal [↗](#)



View related articles [↗](#)



View Crossmark data [↗](#)

RESEARCH ARTICLE



Automatic phytoplankton image smoothing through integrated dual image histogram specification and enhanced background removal method

Mohd Aiman Syahmi Kamarul Baharin^a, Ahmad Shahrizan Abdul Ghani ^a, Normawaty Mohammad-Noor^b, Hasnun Nita Ismail^c and Syafiq Qhushairy Syamsul Amri^a

^aFaculty of Manufacturing and Mechatronics Engineering Technology, Universiti Malaysia Pahang, Pekan, Malaysia; ^bDepartment of Marine Science, Kulliyah of Science, Inter. Islamic University Malaysia, Kuantan, Malaysia; ^cFaculty of Applied Science, University Technology of MARA, Tapah Road, Malaysia

ABSTRACT

Diatom is a dominant phytoplankton and commonly found in oceans or waterways. The captured phytoplankton microscopic images suffer from low contrast and surrounding debris. These images are not appropriated for identification. Integrated dual image contrast adaptive histogram specification with enhanced background removal (DIHS-BR) is proposed to address these issues by automatically removes the background of the phytoplankton image and improves the image quality while cropping phytoplankton cell. DIHS-BR will automatically remove the background and noises. DIHS-BR consists of two major steps, namely, contrast adaptive histogram specification and background removal by means of edge mask cropping. Results demonstrated that DIHS-BR filtered out the image background and left only the required phytoplankton cell image. Noises are minimized, while the contrast and colour of phytoplankton cells are improved. The average edge-based contrast measure (EBCM) of 83.065 demonstrates the best contrast improvement of the proposed methods compared with the other state-of-the-art methods.

ARTICLE HISTORY

Received 22 June 2022
Accepted 14 November 2022

KEYWORDS

Diatom; phytoplankton; image enhancement; edge masking; image smoothing; image brightening; dual-image specification; background removal

Introduction

Diatoms are unicellular microscopic phytoplanktonic organisms that can be found practically in any moist environment (freshwater and saltwater) [1]. Several studies [1–3] have found that a diatom is an important component in the food chain of aquatic ecosystems because it provides food for marine life, such as zooplankton, fish, and shellfish. A diatom ranges in sizes from a few microns to millimetres and could take on thousands of different shapes, such as spheres, ellipses, triangles, and stars. Most of diatom algae could only be observed through microscopes [1, 4].

Digital microscopic image enhancement is a critical issue when dealing with changing lighting conditions [5]. The superiority of digital microscopic images is dependent on a variety of environmental factors, such as relative movement, colour alteration, and uneven lighting conditions. The digital microscopic images of diatom are frequently captured with noise and suffers from low contrast, mixed with floating small objects, or unwanted particles. In addition, the captured images contain many debris especially near the target cells or research subject [6]. In some cases, depending on the magnificent scale, the captured images are blurred as a result of improper focus during the image acquisition process [7]. Examining a fresh phytoplankton under a digital microscope is

difficult, especially when motile microalgae cells are involved [8].

To address these problems, image enhancement is an important preprocessing step before identification and classification of phytoplankton. This step provides an additional attempt to improve the overall image quality or highlights interested properties and characteristics of a related subject matter. These improvement processes can help in strengthening the next image identification process and fulfilling the requirement for a particular analysis [9]. The image enhancement step is required to provide clear image details and improves the overall appearance of the phytoplankton images.

In this work, DIHS-BR consists of two major stages specifically designed to increase the overall quality of an image and retrieves the diatom cell in an output image. In the first stage, the modified dual-image histogram stretching with contrast adaptive histogram specification is implemented to enhance the image quality. The three major components involved in the first step are global contrast modification, local contrast improvement, and colour correction, which are used for image enhancement. In the second stage, the processed image is implemented with a background removal technique in which the edge mask crop technique is applied. In the edge mask crop

step, the background region is removed from the overall image to retrieve only the diatom image cell. Accordingly, diatom cell edges and details are significantly highlighted, and the visibility of the cell structure is incredibly increased. Thus, the proposed DIHS-BR method has the main contributions as follows:

- i Extracting the complete phytoplankton cell from the background areas while retaining the high contrast and colour of the final output image cell.
- ii Minimize the noises and enhancing the edge detail texture of the phytoplankton cell in the final output images.

The rest of this manuscript is ordered as follows: Section 2 describes the related works of the research. Section 3 focuses on the detailed methodology of the proposed DIHS-BR method. Next, the results and discussions that prove the effectiveness and robustness of the proposed method are presented in Section 4. Lastly, Section 5 concludes the proposed work.

Related works

The low contrast microscopic image enhancement algorithm based on a multi-technology fusion method is proposed by Chen et al. [10]. The high and low frequency components of the image are separated to avoid excessive noise while strengthening the images. Furthermore, a low contrast microscopic image improvement was achieved by integrating the Sobel and Laplacian of Gaussian (LoG) operators integrated with contrast limited adaptive histogram equalization method.

Ooi et al. [11] proposed toboggan contrast enhancement (TCE) to enhance of the microscopic colour images. This method enhances the contrast of the microscopic images and reduces the noise level. Gaussian filter is implemented to reduce the image's noise level. However, this filter produces more blurred edges of objects in the image. Toboggan contrast enhancement is used to restore the objects' edges.

Abdul Ghani and Mat Isa [12] introduced a method called dual-image Rayleigh-stretched contrast-limited adaptive histogram specification (DIRS-CLAHS) to improve the underwater image quality by combining global and local contrast stretching based on RGB and HSV colour spaces. Contrast correction mechanism is applied to produce dual-intensity images, which are then combined to generate an enhanced output image. Subsequently, local contrast enhancement is applied to boost the contrast in this image. Next, the colour correction method, which modifies the excessive brightness of an output image, is applied by means of HSV colour model. The proposed method is applied to an underwater image, which suffers from the blue-green colour cast. Based on the sampling,

the proposed method does not significantly eliminate the noise level and floating particles that exist in most phytoplankton images.

Serdar Cakir et al. [13] proposed a method called contrast enhancement of microscopic images using image phase information, which was inspired by the revolutionary design of phase contrast microscopy (PCM). The image enhancement framework in the proposed method transforms changes in the image phase into magnitude variations to improve the image structural details and visibility. The proposed method produces better output images compared with several adaptive histogram equalization-based techniques, but it insignificantly improves dark areas in images because the image details are low.

Abdul Ghani [14] combined a modified Recursive-overlapped Contrast Limited Adaptive Histogram Specification with Dual-image Wavelet Fusion (ROCLAHS + DIWF) to improve contrast underwater images. First, homomorphic filtering was applied to the image to increase the image's colour homogeneity. Second, RO-CLAHS was applied to the image to enhance the edge information before the DIWF method to produce a better natural-looking image. According to the author, this technique achieved the highest entropy value, EME by entropy, and average gradient compared with the state-of-the-art methods.

In 2019, Sonali et al. [15] proposed a method for denoising and enhanced the RGB retinal images using Contrast Limited Adaptive Histogram Equalization (CLAHE). This method employs the CLAHE technique and filters to remove noise and improve the overall digital image contrast, particularly medical images. The CLAHE technique improves the contrast and eliminates artifacts generated by mapping two adjacent grey-scale values to different values [16]. The method improves the overall image to a certain extent. However, the output images tend to have under-enhanced areas in some cases.

Azmi et al. [17] proposed an integrated method called nature-based underwater image with colour enhancement mechanism through fusion of a swarm-intelligence algorithm (NUCE) to improve underwater images with colour distortion neutralization. The method combines both dual image fusion method and swarm-intelligence based means equalization techniques. The result showed that the method is effective in removing the bluish colour cast in the RGB image to a certain level, but inefficient for images with a relatively high blue green colour cast.

Jackson et al. [18] presented a rapid dehazing technique based on dark channel prior and Rayleigh scattering (DCP-RS). The minimum and maximum pixels in each of the three RGB channels of hazy image were determined using the image dehazing approach. Then, Rayleigh scattering theory is used to determine the initial transmission map by modelling a scattering

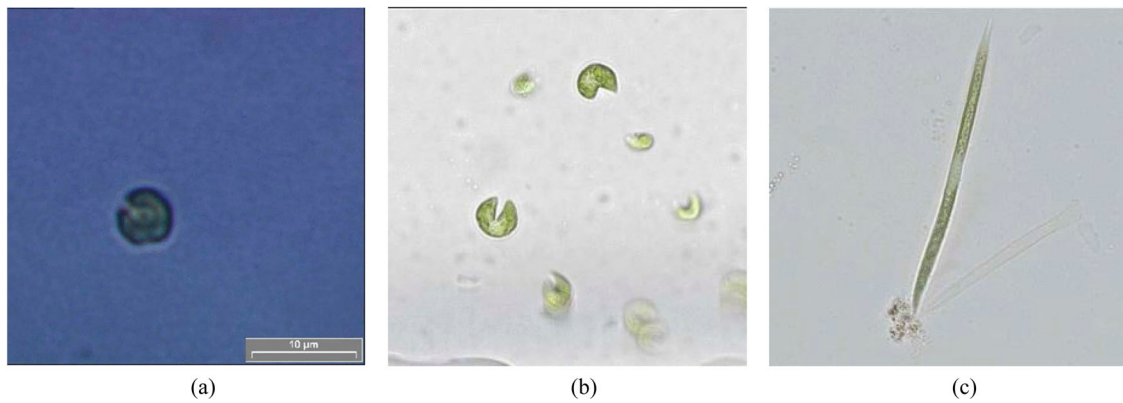


Figure 1. Examples of the microalgae images by Ooi et al. [11] and Borges et al. [4]. (a) low contrast, low brightness, blur, and noise algae image; (b) image with noise, artefacts, and small foreign floating objects; and (c) mucilage in the bottom corner of an elongated single algae image.

coefficient. The image is then refined using a fast-guided filter to correct the erroneous halo edges before being restored using the atmospheric scattering model. The overall output images are improved in terms of haze level. However, a degree of haze element can still be observed in some cases of the output images, especially deteriorated images with a high haze percentage. Figure 1 shows a few original blurred microscopic images with noises and foreign floating objects in the background.

As previously mentioned, most of the captured phytoplankton images suffer from various problems, such as low contrast, deteriorated background colour, low visibility, and high level of noises. These images are hardly processed and unsuitable for the further enhancement and analysis processes, especially for the detection and classification. Foreign floating substances and noises contained in an image might be falsely interpreted as the phytoplankton. This situation leads to wrong detection and classification of the phytoplankton. The following images show the common captured phytoplankton images using a normal microscopic image acquisition device. In the sample images in Figure 2, the captured phytoplankton image cells have diverse backgrounds and contrast, which affect their visibility and identification. Some of the phytoplankton are captured in dark background areas with

low contrast (Figure 2(a)) in which the cells are hardly seen and differentiated from the background. In certain cases, the captured images are blur (Figures 2b and d), and some are captured in a high level of noise in which the cell edges are hardly differentiated (e.g. Figure 2c). These problems lead to unsuccessful or low rate of detection and classification processes of phytoplankton.

Manigandan and Vaithyanathan [19] proposed underwater image enhancement with colour constancy and dehazing based on depth estimation. The method improves the overall image visibility because the objects in the image are better differentiated. However, excessive colour distortion occurs in certain areas, especially when the original image is dark. Liu et al. [20] combined the physical model and generative adversarial network for the improvement of underwater images. Fard et al [21] introduced a novel strategy in histogram of oriented gradients, which can calculate dips in different directions. These conducted experiments show an adequate enhancement of the contrast and colour of the output images. Nevertheless, the processed images produce haze, resulting in limited visibility, because the captured objects in the image are distanced from the camera.

One of the interesting techniques for image dehazing and colour correction is the integration with the

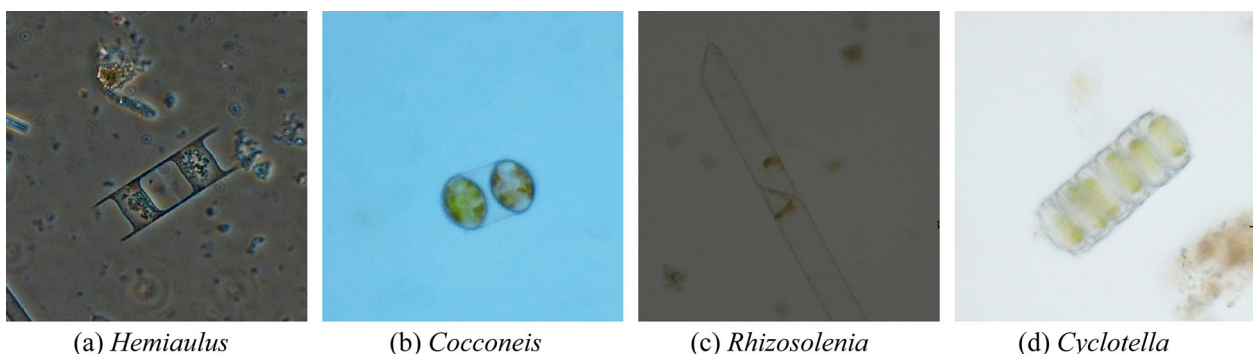


Figure 2. Sample of various phytoplankton images.

neural network approach. Li et al. [22] introduced a deep convolutional neural network (CNN) for single image dehazing called a perception-inspired single image dehazing network with refinement (PDR-Net). Yang et al. [23] proposed a method called the Region Detection Network model, which reflects the regional detection of a single blurry image. The findings reveal that the neural network outperforms conventional methods in estimating ambient light and transmission. Nevertheless, the CNN method's disadvantage is that it requires a large image dataset to process and achieves a successful output [24].

Methodology

In this study, the phytoplankton are collected from various sources, including from the coastal waters of Pahang [25] and the University of California Santa Cruz phytoplankton database [26]. The collected samples are observed under digital microscope Nikon DS-Ri1, and the images are taken at a total magnification of 400× and 200× assisted with Nikon Element Imaging Software. Approximately 100 phytoplankton sample images with an original resolution of 1280 × 1024 pixels were captured for this study.

The experimental work has been conducted using MATLAB R2021a installed on a Microsoft Windows 10 operated computer with Intel Core i5, 2.90 GHz, 8 GB RAM. According to the experiment, the average total time taken to run the whole algorithm for a single image with a size of 1280 × 1024 pixels is around 2 s. The experimental results show that the proposed algorithm is suitable for practical uses because the resultant images are of good quality, and the phytoplankton cells are highly visible and separated from the background.

Introduction

The captured phytoplankton images have a high noise level and contain foreign floating particles. These problems could be solved by means of background removal, which is included in the proposed DIHS-BR method. Background removal by edge mask cropping is designed and integrated in the proposed DIHS-BR method to improve the image quality by reducing the noise level and eliminating the floating particles that impede phytoplankton cell detection. The final output image of this proposed method will have only the particular diatom cell shown in Figure 3 and the final output images of the proposed method in Section 4.

The proposed DIHS-BR method algorithm is designed with two main processes. The first step, namely, contrast adaptive histogram specification, is implemented to enhance the overall input image contrast and results in significant quality improvement. Meanwhile, the second step, namely, background

removal technique, refers to the extraction of the phytoplankton cell from the background image by edge-mask cropping. From the first step, the applied enhancement process yields additional affects because it has significantly reduced the noise and produces homogeneous illumination around the phytoplankton cell. Consequently, a better platform for the cell extraction and background removal could be provided for the next process. Nevertheless, in the proposed DIHS-BR method, only the required phytoplankton cell image appears in the final output image for the cell identification. In addition, the colour correction technique has been included in the proposed method to boost the colour of the phytoplankton algae.

In comparison with previous studies [10–20], some methods do not significantly reduce the noise from the raw input image and results in interference between the noise and the phytoplankton cell in the final output image. Consequently, the phytoplankton cell could not be significantly identified. In addition, certain previous methods do not integrate the pre-processing step and focus on the basic individual process, such as contrast enhancement, denoising, or dehazing.

Figure 3 illustrates the proposed methodology of the DIHS-BR method. Brief descriptions of the applied steps are as follows:

- Step 1: The original input image is applied with the modified dual image contrast adaptive histogram specification technique to improve the overall image quality.
- Step 2: Implementation of the improved haze removal technique to remove the apparent noises and haze in the image.
- Step 3: Integrated image brightening and edge masking to highlight the edge of the diatom cell with improved background removal approach of diatom cell.
- Step 4: Unsupervised image contrast enhancement.

Dual image contrast adaptive histogram specification for the overall image enhancement

Image enhancement, which is set up as a pre-processing phase, is an important step before the edge mask cropping. This step provides the image with a fine contrast by increasing the visibility of the region of interest. In this step, the input image histogram is divided into two regions based on the average intensity value. Both histogram regions are stretched to the whole 255 dynamic ranges of the 8 bit image, producing two different intensity images, namely, over-enhanced and under-enhanced images.

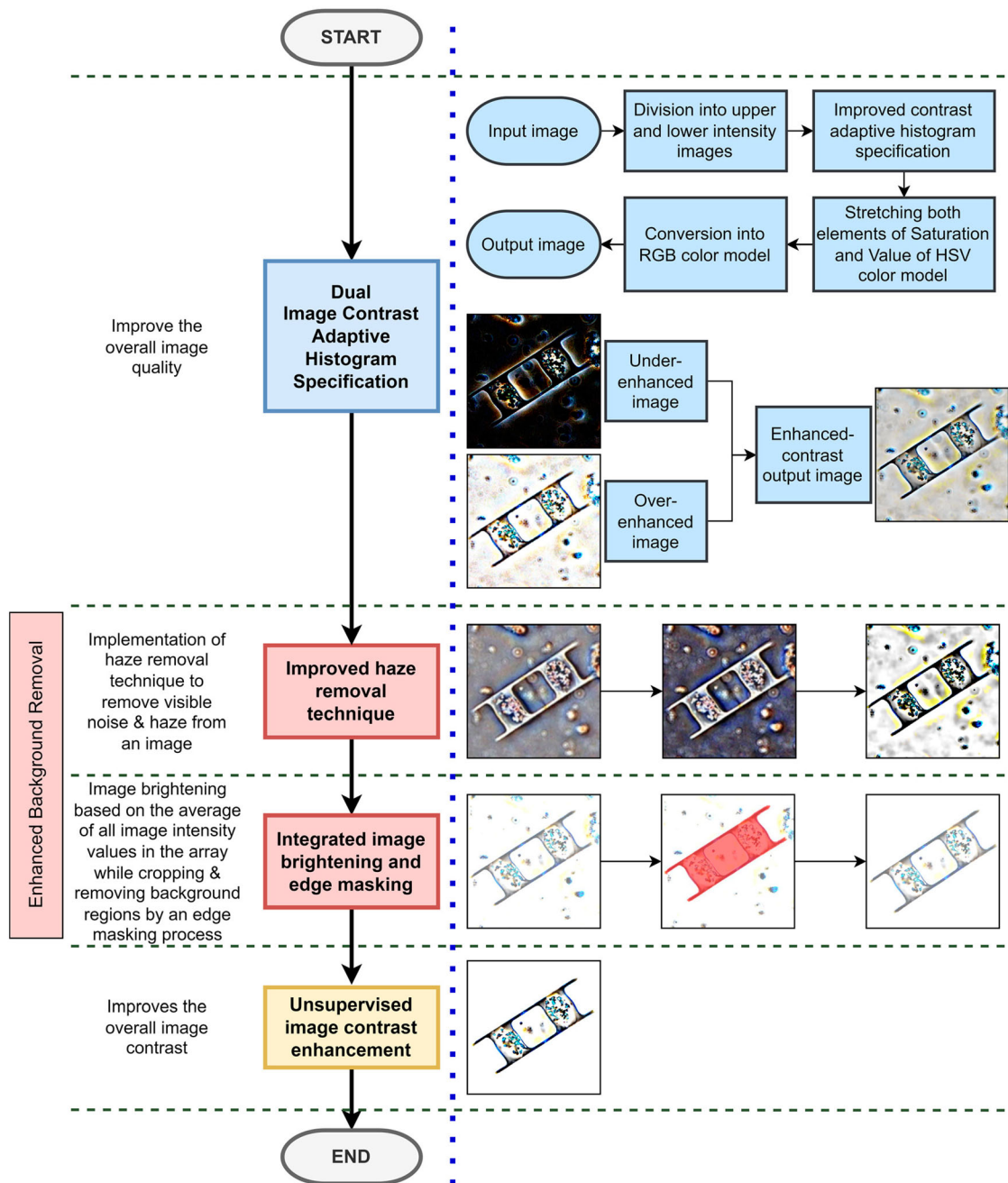


Figure 3. Illustration of the proposed DIHS-BR method.

The average intensity value of an image with n number of pixels, x at the position of (i, j) , could be calculated by using Equation (1).

$$i_{average} = \frac{\sum_{ij}^n x_{ij}}{n} \quad (1)$$

The stretching process is applied as per Equation (2).

$$P_{out} = (P_{in} + i_{min}) \left(\frac{o_{max} + o_{min}}{i_{max} + i_{min}} \right) + o_{min} \quad (2)$$

where P_{in} and P_{out} are the input and output pixels, respectively. The minimum and maximum intensity values of the input and output images are denoted as i_{min} , i_{mid} , o_{min} , and o_{max} .

The obtained over- and under-enhanced images are then applied with contrast adaptive histogram specification in which the histogram distribution is specified to follow the Rayleigh distribution map wherein the concentration of the image pixels is at the middle areas of the histogram. The image is then converted from red-green-blue (RGB) into an HSV colour model for the colour correction. The saturation (S) and value (V) components of the colour model are stretched to increase the colour dynamic range of the output image before it is converted back into an RGB colour model. The following figure simplifies the step applied in the contrast adaptive histogram specification Figure 4.

The mapping of the intensity distribution follows the Rayleigh distribution, which is a bell-shaped

intensity distribution in which the image pixels concentrate more in the middle range of the intensity values. The probability distribution function (PDF) and cumulative distribution function (CDF) of the Rayleigh distribution are represented in Equations (3) and (4), respectively. x is the input pixel, and α is the Rayleigh distribution parameter.

$$PDF_{Rayleigh} = \left(\frac{x}{\alpha^2}\right)e^{(-x^2/2\alpha^2)} \quad (3)$$

$$CDF_{Rayleigh} = 1 - e^{(-x^2/2\alpha^2)} \quad (4)$$

Furthermore, colour correction is the last step in implementing the contrast adaptive histogram specification. The image is first converted into an HSV colour model before the channels are decomposed. The most influenced channels of saturation (S) and value (V) are stretched to the entire dynamic range of the colour model to widen its capability in distributing the image pixel throughout the image dynamic range of a particular colour model.

In this case, the midpoint i_{mid} of the S and V components are calculated using Equation (5), whereas i_{min} and i_{max} represent the minimum and maximum intensity values of the S and V components, respectively.

$$i_{mid} = \left(\frac{i_{min} + i_{max}}{2}\right) \quad (5)$$

The histograms of S and V are then stretched depending on their midpoints. The histogram outputs should follow Equation (6) of the Rayleigh-stretched histogram.

$$Rayl. - stretched = \frac{P_{in}O_{max} - P_{in}O_{min} - i_{min}O_{max} - O_{min}i_{max}}{\alpha^2(i_{max} - i_{min})^2} \cdot \exp\left[\frac{[P_{in}O_{max} - P_{in}O_{min} - i_{min}O_{max} - O_{min}i_{max}]^2}{2\alpha^2(i_{max} - i_{min})^2}\right] \quad (6)$$

The obtained average pixels values of the stretched histograms, I_{avg} , is applied to integrate the lower-stretched and upper-stretched histograms of the S and V components, as shown in Equation (7). $I_{LS}(i, j)$ and $I_{US}(i, j)$ are the intensity values for the lower-stretched and upper-stretched histograms at pixel's

positions (i, j) , respectively.

$$I_{avg} = \left(\frac{I_{LS}(i, j) + I_{US}(i, j)}{2}\right) \quad (7)$$

In the final step, the H, S, and V components are composed to generate an image in the HSV colour model, which is then converted into the RGB colour model. Accordingly, an improved output image is produced, as shown in Figure 5(b). In the aforementioned figure, the phytoplankton algae cell is more visible, and the overall image has better contrast and colour with homogeneous illumination. In addition, 3D RGB representation shows a wide distribution of the intensity pixels of the image after implementing such a process. The output image in this step is further processed for smoothing based on the background removal technique.

Enhanced background removal

In the experiment, the low-light output image produced from the previous step contains noises and floating particles. These noises and floating particles might be mixed with micro-size phytoplankton itself. Consequently, the detection and identification processes cannot be run, or the successful rate in the phytoplankton detection might be low. To address this problem, the background removal technique is integrated in the main process, whereas the haze removal and edge masking steps are applied.

Improved haze removal technique

Edge detection of a phytoplankton image is the most important process in the pre-processing of the background removal step. Determining the edge or border of a phytoplankton results in a higher successful identification rate of its features. Furthermore, the characteristics may be correctly identified. Consequently, the type and family group of phytoplankton would be easier to be classified.

The proposed DIHS-BR method is designed to address this objective. The output image from the previous step is first inverted into a negative image and boosted with the enhancement process through the haze removal technique before the image is brightened to smoothen the background areas. The image is then edge mask cropped to reveal the image background. Subsequently, the output image is reinverted to a positive image. Thus, only the phytoplankton cell image is left.

The enhanced haze removal technique for a low-light image consists of three major steps. The image is first inverted into a negative image based on Dong et al. [27] to observe how lowlight areas in the contrast adaptive histogram specification image appear hazy, as described in Equation (8).

$$R^c(x) = 255 - I^c(x) \quad (8)$$

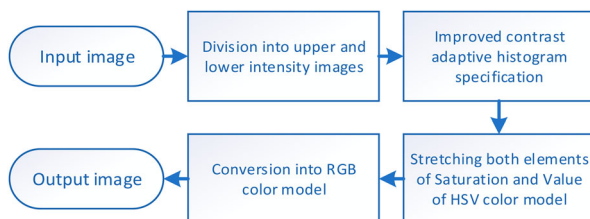
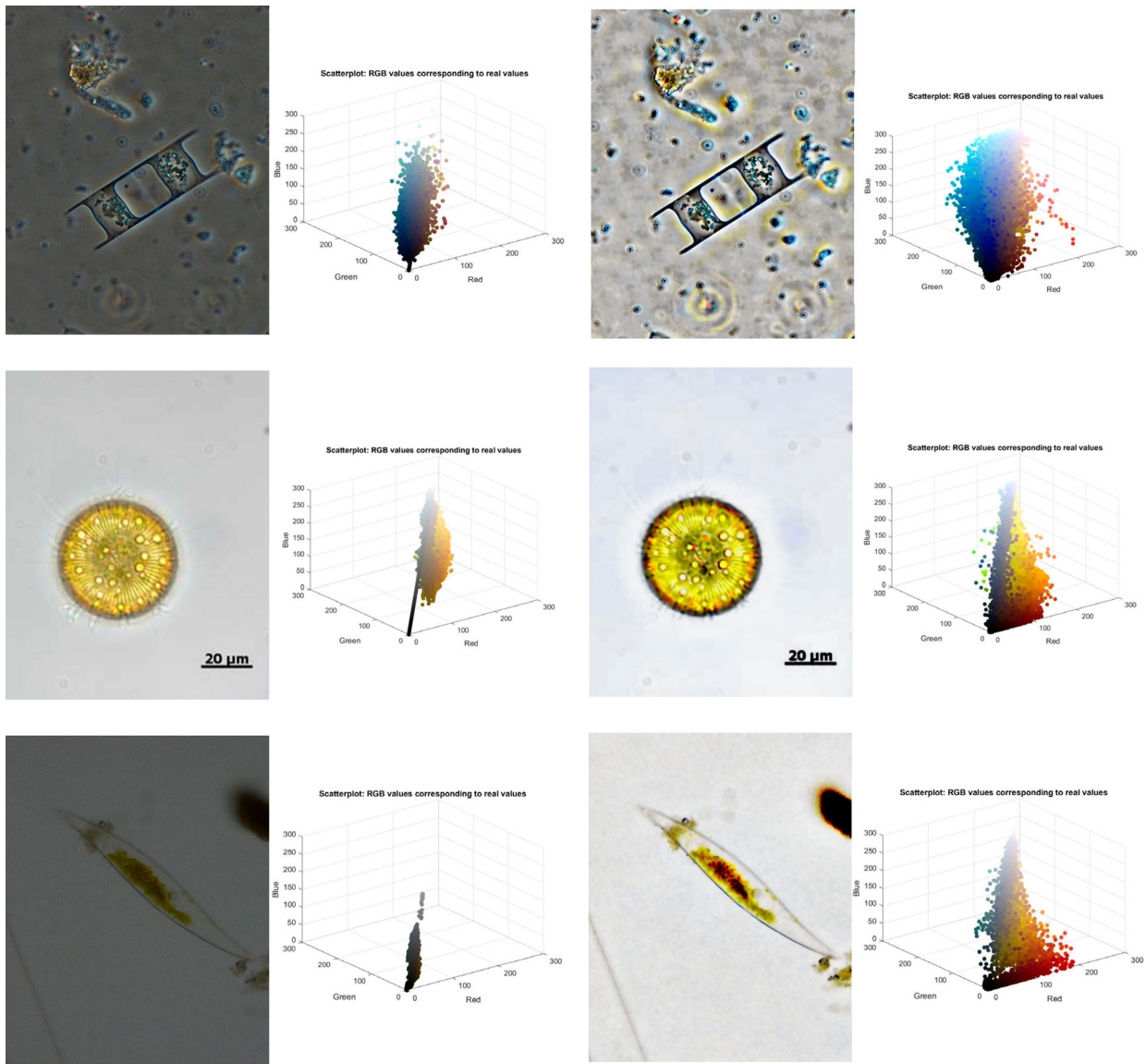


Figure 4. Illustration of the steps involved in the applied improved contrast adaptive histogram specification.



(a) Original image

(b) Improved contrast adaptive histogram specification

Figure 5. (a) Original image with 3D RGB colour representation; (b) output image after the implementation of the improved contrast adaptive histogram specification with 3D RGB colour representation.

where $I^c(x)$ is the intensity of a colour channel of pixel x for a particular low-light input image I , $R^c(x)$ refers to the inverted intensity image R , and c indicates the colour channel, which refers to the RGB in this case. Figure 6(b) shows a sample of an inverted low-light image after it has been inverted. Next, the inverted image is dehazed by applying the dehazing algorithm, as described by Equation (9) [28].

$$R(x) = J(x) \times t(x) + A(1 - t(x)) \quad (9)$$

where A denotes the total amount of light emitted by the atmosphere on a global scale, $R(x)$ denotes the brightness of the pixel x captured by the microscope camera, $J(x)$ is the original object's or scene's intensity, and $t(x)$ indicates the percentage of light emitted by objects that is captured by the microscope camera. According to this equation, the haze removal

algorithm highly relies on the estimation of A and $t(x)$ of the captured image with intensity $I(x)$ to recover $J(x)$ from $I(x)$. The result is shown in Figure 5(c).

The inversion operation described in Equation (8) is repeated to create an enhanced output image. Accordingly, an improved output image is created after inversion to negative image and dehazing algorithm, as shown in Figure 6(d).

Integrated image brightening and edge masking

Next, the integrated brightening process and edge masking of the image is conducted to increase the visibility of the diatom edges while eliminating small unwanted particles. The image brightening process is based on the mean value of all image intensity values in the array. Figure 7 shows a sample of the image after the implementation of image brightening.

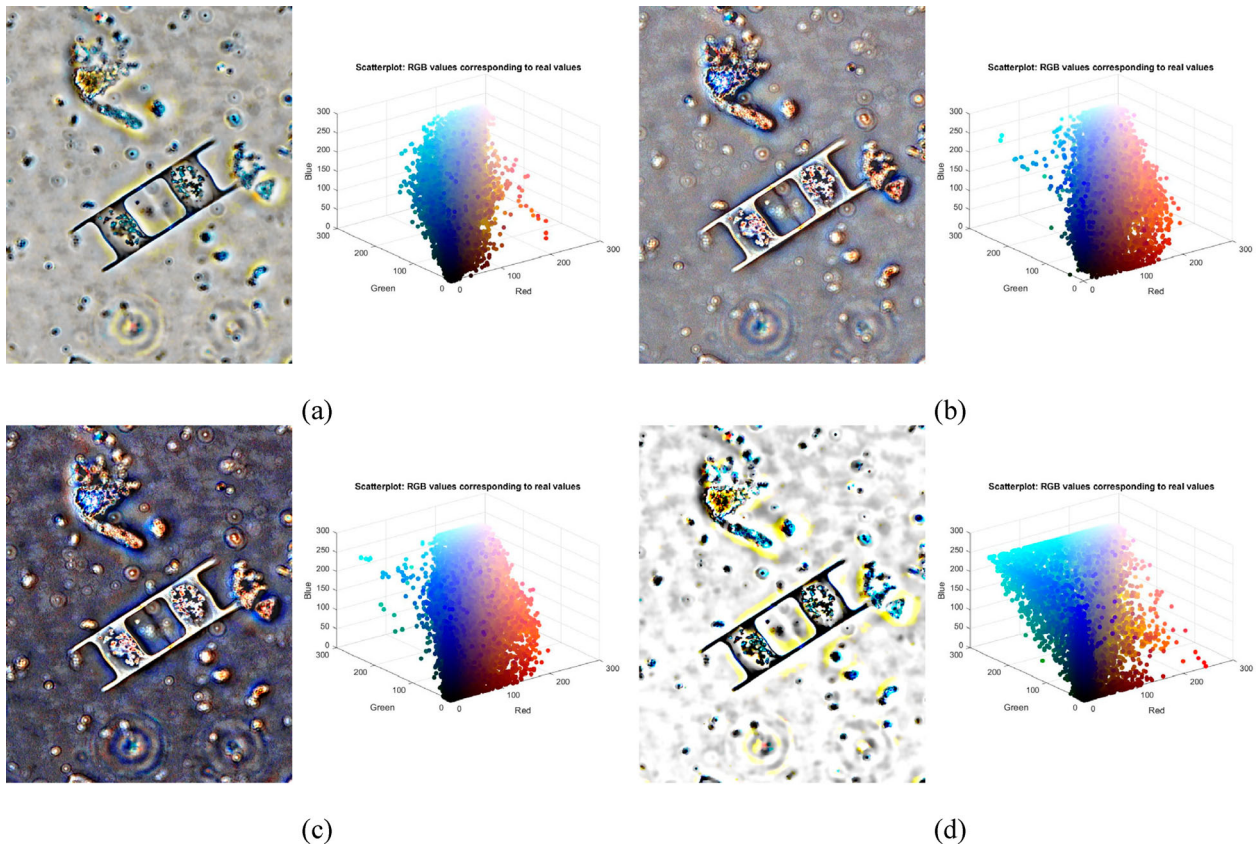


Figure 6. (a) Contrast adaptive histogram specification; (b) inverted image; (c) dehazing algorithm; and (d) output image after the re-inversion algorithm.

The output image from the previous step is applied with automatic marking of the region of interest (ROI). In this case, the ROI refers to the phytoplankton cell. The edge of the ROI will be identified and highlighted before the phytoplankton is cropped, and the background of the image (aside from the cropped phytoplankton cell) will be converted into a white area (replaced with the highest intensity value of 255) in which the background will be seen as white. This white background areas are prepared for the next identification process.

The background removal method begins with the implementation of the morphological operators to reduce or eliminate dark details, resulting in a bright output image; the image’s bright details are toned down during the erosion operation [29]. The main purpose of morphological process is to highlight the ROI of the image and separate it from the background region. Binary dilation could be represented by Equation (10).

$$A \oplus E = \{z | (\hat{E})_z \cap A \neq \emptyset\} \quad (10)$$

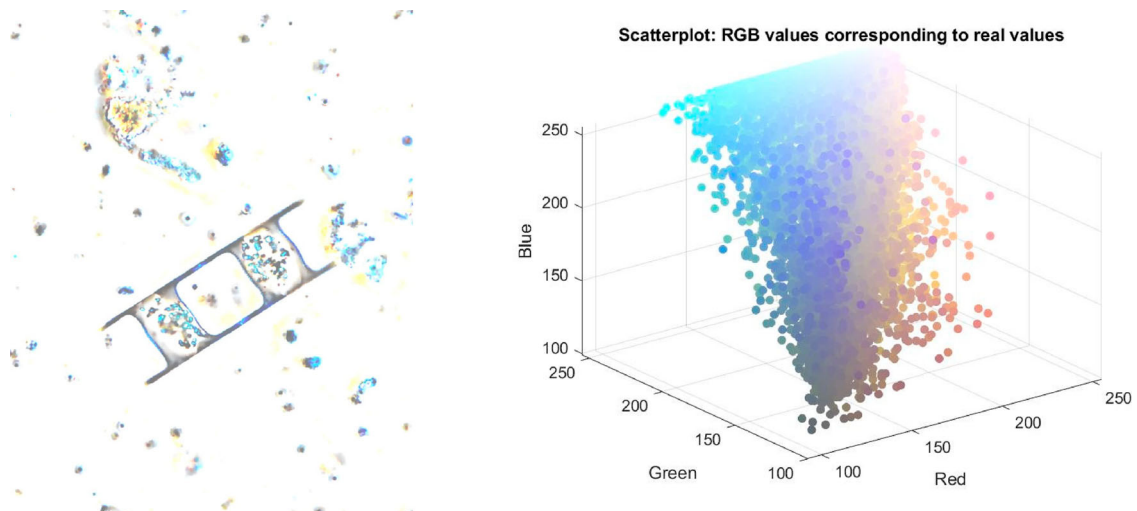


Figure 7. Diatom image after the implementation of image brightening.

where \hat{E} refers to the structural element of the E reflection. Specifically, it is the collection of pixel positions z in which the reflected structuring element overlaps with the foreground pixels in A when translated to z [30].

$A \ominus E$ is defined by Equation (11) for the binary erosion of A by E .

$$A \ominus E = \{z | E_z \subseteq A\} \quad (11)$$

where z is the set of pixel locations where the structuring element translated to location overlaps only with the foreground pixels in A .

A flat morphological structuring element is required for the morphological dilation and erosion operations [31]. This element creates a structuring element type, which is specified by a particular shape to highlight the ROI and object edges. The shape used in the function refers to the *disk*. Meanwhile, a positive R parameter, which specifies the radius, creates a flat, disk-shaped structuring element in the applied image. The analysis of the diatom image shows that the optimal value of R is one, which refers to the minimal parameter value. Figure 8 illustrates the analysis sample result of *dilation* and *erosion* functions to determine the best R value. According to the analysis, the foreign particles are totally unmarked when the radius R is equal to one.

The previous output image is further improved in terms of edge masking to increase the sharpness of the marked edges. This result could be observed in Figure 9. The produced uneven edge mask is smoothed by eliminating all linked components from the red colour of the highlighted edge mask within a specific range. Consequently, another binary image with smooth highlighted ROI edges of the phytoplankton diatom cell that fulfil the criteria is produced, as shown in Figure 9(b).

Next, the mask cropping process is applied in the background removal step to crop and remove the background regions. Consequently, only the ROI for the diatom cell remains in the final output image. The cropping process extracts all connected components from a binary image highlighted in red colour and return a binary image containing the only diatom cell (ROI). Figure 10(a) presents samples of the phytoplankton image highlighting process. Figure 10(b) shows the phytoplankton images of the

diatom after the mask cropping process, in which the only diatom cell image is produced.

In several cases, when more than one cell of phytoplankton is in a single image, the background removal method will extract both or all of them as long as the cells are connected or side by side, as shown in Figures 11(a) and (b). Furthermore, the designed background removal method also could extract phytoplankton from the background, although the cell shape is not complete or only half complete, as shown in Figure 11(c).

In the final step, an improved contrast modification is applied by adjusting the image contrast. This step adjusts the image's contrast by considering that 1% of the dynamic range values are saturated at low and high intensities of the diatom cell image. This step improves the overall image contrast, as shown in Figures 12–16.

Results and discussions

Five out of 100 diatom images are chosen to verify and prove the effectiveness and the reliability of the proposed DIHS-BR method in enhancing the phytoplankton image and removing the unwanted background, especially in preparing the only diatom image for the detection and classification process, as shown in Figures 12–16. Qualitative and quantitative evaluations are conducted to ensure that the proposed method can preserve the shape and details of the phytoplankton compared with the other methods. In terms of image processing, visual observation (qualitative evaluation) emphasizes the overall image quality. In this work, quantitative measurement should support qualitative impressions. However, since the main purpose of this research work is to extract the phytoplankton cell while removing the background and other foreign particles, the proposed method is apparently reducing the quantitative image details (measured through entropy and universal image quality index (UIQI)) as the image background except the phytoplankton cell are removed. Meanwhile, the mean squared error (MSE) will increase, and the peak signal-to-noise ratio (PSNR) will decrease because the extracted output image is different from the input image due to the removal of the output image's

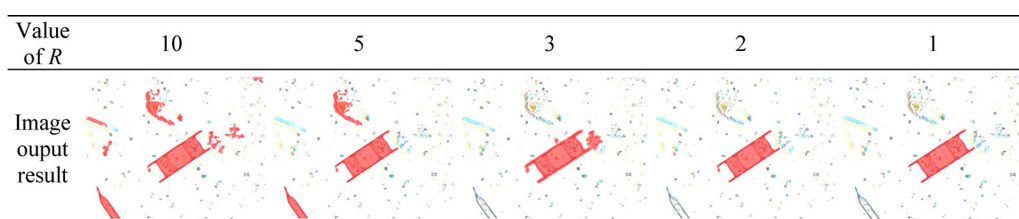


Figure 8. Resultant images of dilation that are applied after the erosion with different values of R .

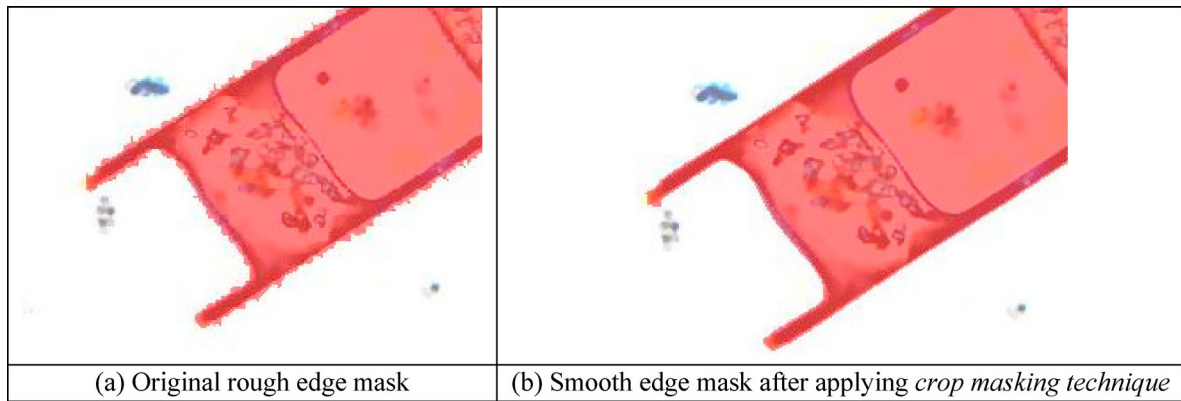


Figure 9. Comparison of the edge masks before and after applying the *crop masking technique*.

background. Nevertheless, the quantitative evaluations are conducted in this work are for the purpose of comparison with other related methods. The primary comparative measurement to prove the effectiveness of the proposed DIHS-BR method is still the qualitative evaluations.

The proposed DIHS-BR method is to enhance and extract the phytoplankton from the background. All of the reference papers within these areas focus on individual work such as enhancement of underwater images, enhancement of microscopic images, and some papers are related to noise removal and dehazing images. Most of the methods compared with the proposed DIHS-BR method use contrast and smoothing the image at the same time in comparison to the resultant image, but our method has extra steps that are background removal technique in which the edge mask crop technique is applied, in which the other methods does not have.

Qualitative evaluation

The dark images of *Hemiaulus*, *Leptocylindrus*, and *Thalassionema* suffer from low intensity because the phytoplankton cells are hardly seen and differentiated from the background (Figure 12 15 and 16). In addition, foreign floating elements can be observed in the original images, casting shadows on the main phytoplankton cells. The images of interested phytoplankton cells are successfully enhanced and become more visible when the first major step of enhanced contrast adaptive histogram specification is applied. After the masked-cropping background removal, the phytoplankton successfully separated from the background to produce a single phytoplankton cell in the output image. The proposed method has increased the visibility inside the phytoplankton cell and significantly visualizes the phytoplankton shape. The colour of the extracted cell is significantly improved.

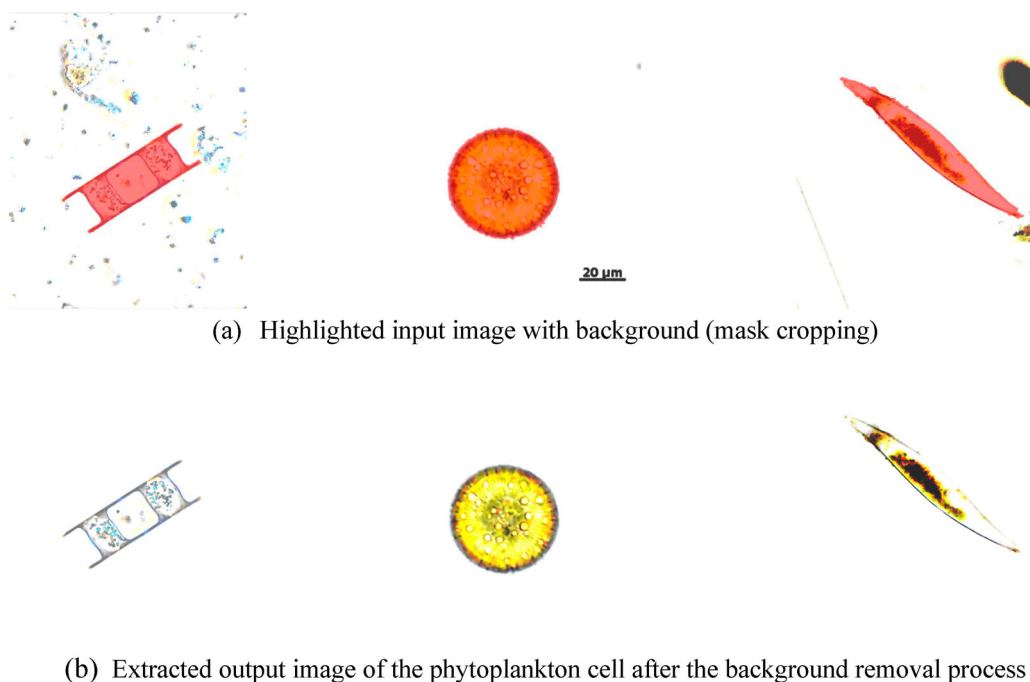


Figure 10. (a) Highlighted input image with edge mask crop; (b) output image after edge cropping.

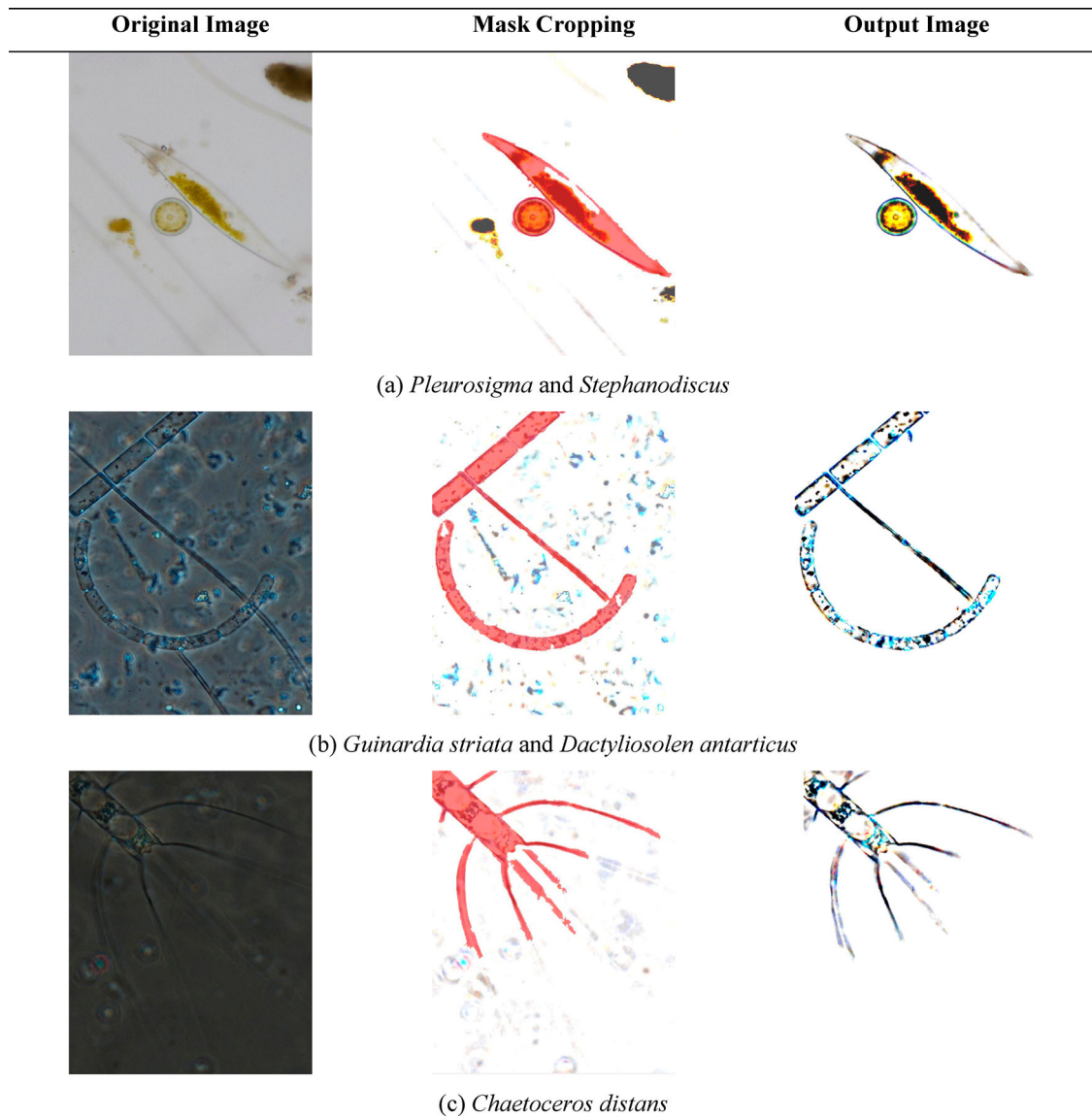


Figure 11. Image of multiple phytoplankton for the background removal.

Similar effects could be observed in the bright images of *Stephanodiscus* and *Cyclotella*, as shown in Figures 13 and 14. The proposed method has successfully improved the overall image contrast and colour because the images of the phytoplankton cells become highly visible. In addition, the shape of the phytoplankton cells is retained and improved

compared with the original images. A sharp edge could be observed in the final output image, which might increase the degree of detection and classification rate.

In the second experiment, the proposed DIHS-BR method is applied on different scales of phytoplankton. The results show that the DIHS-BR method has

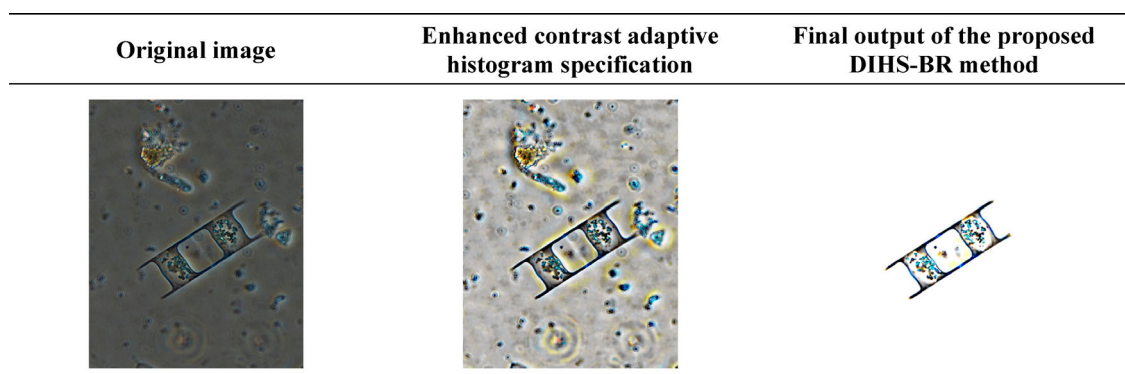


Figure 12. Image of phytoplankton *Hemiaulus*.

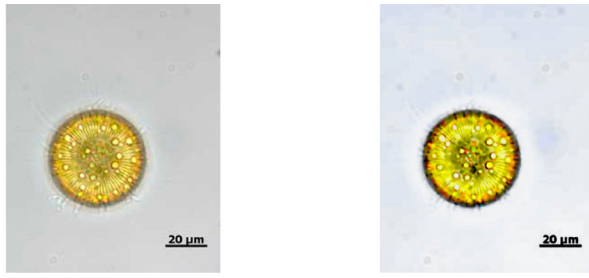


Figure 13. Image of phytoplankton *Stephanodiscus*.

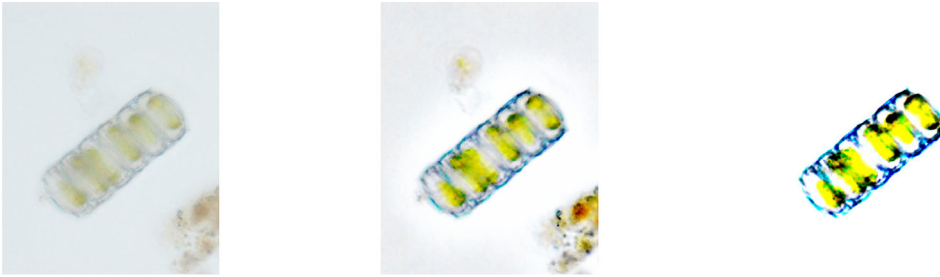


Figure 14. Image of phytoplankton *Cyclotella*.

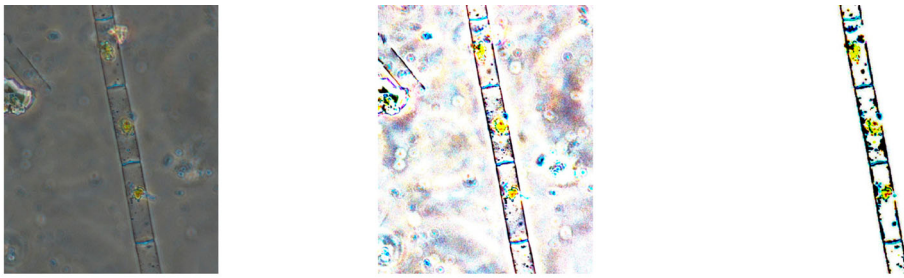


Figure 15. Image of phytoplankton *Leptocylindrus*.

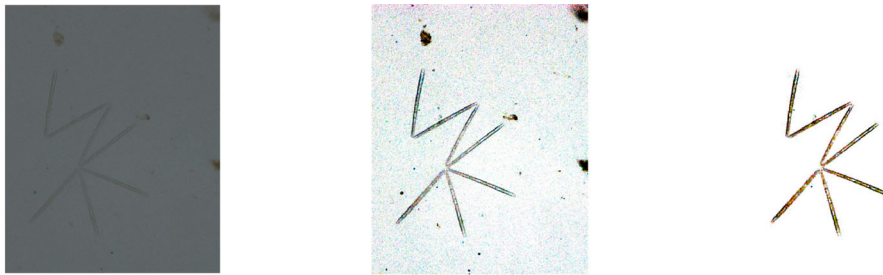


Figure 16. Image of phytoplankton *Thalassionema*.

successfully extracted the phytoplankton cells and eliminated the background while enhancing the image, although the range occupied by phytoplankton in the image is small, as shown in Figure 17.

Quantitative evaluation: objective performance evaluation

In addition to the qualitative evaluation, quantitative performance evaluations are used to compare the output images between state-of-the-art methods. In

this work, the output images are evaluated in terms of entropy, MSE, PSNR, absolute mean brightness error (AMBE), edge-based contrast measure (EBCM), and UIQI. Among these quantitative evaluations, EBCM might be the best quantitative evaluation that represents the quality improvement of the proposed method. Nevertheless, the human visual system (HVS) provides the best evaluation of the effectiveness of the proposed DIHS-BR method.

Entropy characterizes the image information or image details, and a higher value of entropy represents

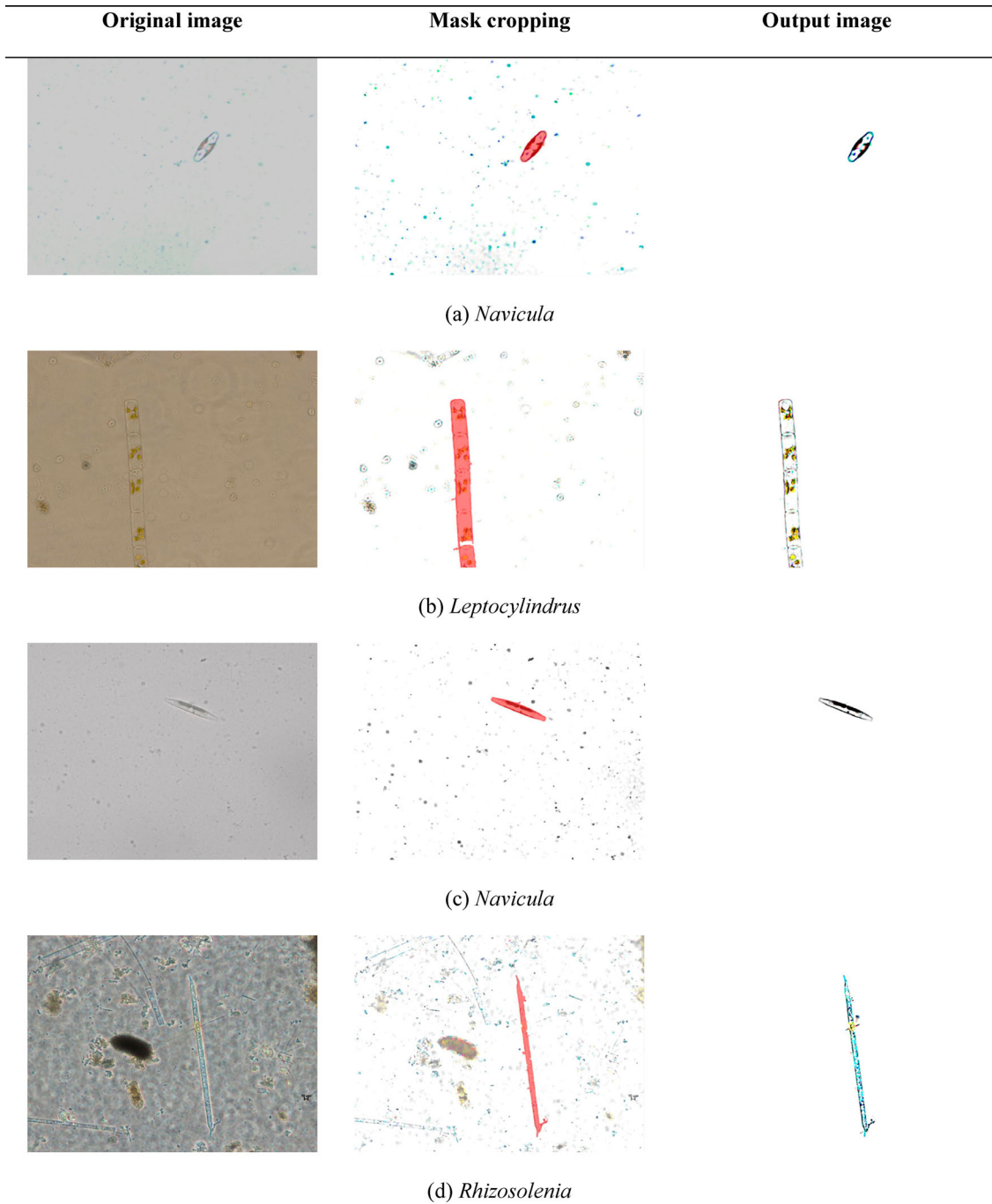


Figure 17. Image of different scales of phytoplankton for the background removal.

a better image quality. Entropy, $H(X)$, of the phytoplankton images is obtained using the following formula:

$$H(X) = - \sum_{x=1}^k p(x) \log_2 p(x) \quad (12)$$

where $p(x)$ specifies the probability distribution function of the image at state x (pixel), while k denotes to the number of grey level [32].

MSE is the average of the square of the difference between the enhanced image, $(r'(i,j), g'(i,j), b'(i,j))$ and the original image $(r(i,j), g(i,j), b(i,j))$. The lower the MSE, the closer the enhanced image is to the

original [33].

$$MSE = \frac{1}{MN} \sum_{i=0}^{M-1} \sum_{j=0}^{N-1} \left[\begin{array}{l} (r(i,j) - r'(i,j))^2 + \\ (g(i,j) - g'(i,j))^2 + \\ (b(i,j) - b'(i,j))^2 \end{array} \right] \quad (13)$$

PSNR, which is measured in decibels (dB), is used to measure the quality of the reconstructed image. In the PSNR analysis, the greater the PSNR value, the better the reconstructed image. The formula for calculating the PSNR value is as follows:

$$PSNR = 20 \log_{10} \frac{(2^B - 1)}{\sqrt{MSE}} \quad (14)$$

where B represents the bits per sample.

AMBE refers to the difference between the mean intensity levels of the enhanced and the original images, and it is mainly used to assess the preservation of brightness in processed images following contrast augmentation [34]. AMBE can be defined as follows:

$$\text{AMBE} = |I(y) - I(x)| \quad (15)$$

where $I(y)$ is the mean intensity level of the enhanced image, and $I(x)$ is the mean intensity level of the original image. A low AMBE value indicates better preservation of the method.

UIQI [35] is defined as a comprehensive reference image quality measurement that evaluates the overall quality as the combination of contrast distortion, luminance distortion, and loss of correlation through Equation (16).

$$\text{UIQI} = \frac{\sigma_{xy}}{\sigma_x \sigma_y} \cdot \frac{2\mu_x \mu_y}{\mu_x^2 + \mu_y^2} \cdot \frac{2\sigma_x \sigma_y}{\sigma_x^2 + \sigma_y^2} \quad (16)$$

where μ_x and μ_y , are the mean values of images x and y , respectively; and σ_x , and σ_y denote the standard deviations of images x and y , respectively. These components are multiplicatively combined to generate a final quality score. UIQI takes values in the interval of $[-1, 1]$. The higher values of the measurement indicates better image enhancement.

Meanwhile, EBCM is based on the observation that the human perception mechanisms are susceptible to contours or edges [36]. The formula for calculating

the EBCM value is given by Equation (17).

$$\begin{aligned} \text{EBCM} |f(x, y)| &= \sum_{x=1}^M \sum_{y=1}^N C(x, y) / \sum_{k=0}^{L-1} H(k) \\ &= \frac{1}{MN} \sum_{x=1}^M \sum_{y=1}^N C(x, y) \end{aligned} \quad (17)$$

where $C(x, y)$ is the edge value at pixel (x, y) .

Table 1 shows the dataset of the quantitative evaluation of the proposed method and several state-of-the-art methods for the images in Figures 18–20 in terms of entropy, MSE, PSNR, AMBE, UIQI, and EBCM. All of the quantitative analysis in Table 1, except EBCM, shows that the proposed DIHS-BR method does not fulfil the performance measures because the final output of the image contains only the diatom algae cells that are different from the original image. The proposed DIHS-BR is expected to eliminate all noises and background areas while extracting the only phytoplankton cell. Removing all unwanted background results in a larger difference between the output and the original images, as most quantitative measurement does.

For instance, the RO-CLAHS + DIWF method yields the highest value of MSE, PSNR, and AMBE, indicating that the image enhancement process has successfully increased the contrast and brightness of the image (Figures 18 and 20). However, based on the output image, this method cannot eliminate the background areas while eliminating the noises in the image. Meanwhile, the proposed DIHS-BR method has successfully eliminated the noises and unwanted floating particles while removing the background areas. In terms of EBCM, the proposed method produces the highest value compared with the other methods because it

Table 1. Quantitative evaluation of the different methods for the phytoplankton diatom image in Figures 18–20.

Figure	Method	Qualitative performance measures						Processing time (s)
		Entropy ↑	MSE ↓	PSNR ↑	AMBE ↓	UIQI ↑	EBCM ↑	
<i>Cyclotella</i>	DIRS-CLAHS	2.864	2074	14.963	35.621	0.183	81.352	0.956
	CLAHE	6.294	1945	15.241	40.974	0.258	75.671	0.611
	PCM	6.978	2450	14.239	41.110	0.143	60.061	1.882
	NUCE	7.460	2887	13.526	34.714	0.161	54.680	26.580
	DCP-RS	6.408	1002	18.120	15.902	0.397	80.217	0.574
	RO-CLAHS + DIWF	6.757	856	18.803	4.171	0.247	78.162	1.309
	TCE	6.924	1591	16.114	32.668	0.182	69.774	0.869
	DIHS-BR	0.427	2747	13.742	46.503	0.032	82.621	1.578
	DIHS-BR	3.546	8305	8.937	82.844	0.275	82.431	0.964
<i>Cocconeis</i>	DIRS-CLAHS	6.382	707	19.633	19.980	0.340	58.890	0.585
	CLAHE	7.078	1254	17.146	19.976	0.187	42.849	1.849
	PCM	7.329	2149	14.807	1.708	0.167	44.262	36.400
	NUCE	6.509	4167	11.932	56.067	0.367	82.108	0.569
	DCP-RS	6.841	2695	13.825	40.390	0.245	80.683	0.957
	RO-CLAHS + DIWF	6.809	1502	16.363	30.257	0.298	80.584	0.842
	TCE	0.284	9961	8.148	93.500	0.0319	83.828	1.548
	DIHS-BR	3.129	3358	12.870	54.090	0.258	82.283	2.183
	DIHS-BR	7.016	2352	14.415	42.442	0.344	58.488	0.566
<i>Hemialus</i>	DIRS-CLAHS	7.633	3833	12.294	42.822	0.200	51.798	2.547
	CLAHE	6.944	1901	15.339	36.665	0.382	53.229	67.381
	PCM	6.470	550	20.722	18.213	0.571	82.060	1.358
	NUCE	6.470	550	20.722	18.213	0.571	82.060	1.358
	DCP-RS	7.047	524	20.931	4.840	0.376	78.447	0.928
	RO-CLAHS + DIWF	7.003	2793	13.700	46.611	0.268	55.309	0.987
	TCE	0.927	3953	12.161	57.590	0.086	82.364	1.509
	DIHS-BR	0.927	3953	12.161	57.590	0.086	82.364	1.509
	DIHS-BR	0.927	3953	12.161	57.590	0.086	82.364	1.509

Note: The value in bold represents the best result from the comparison.

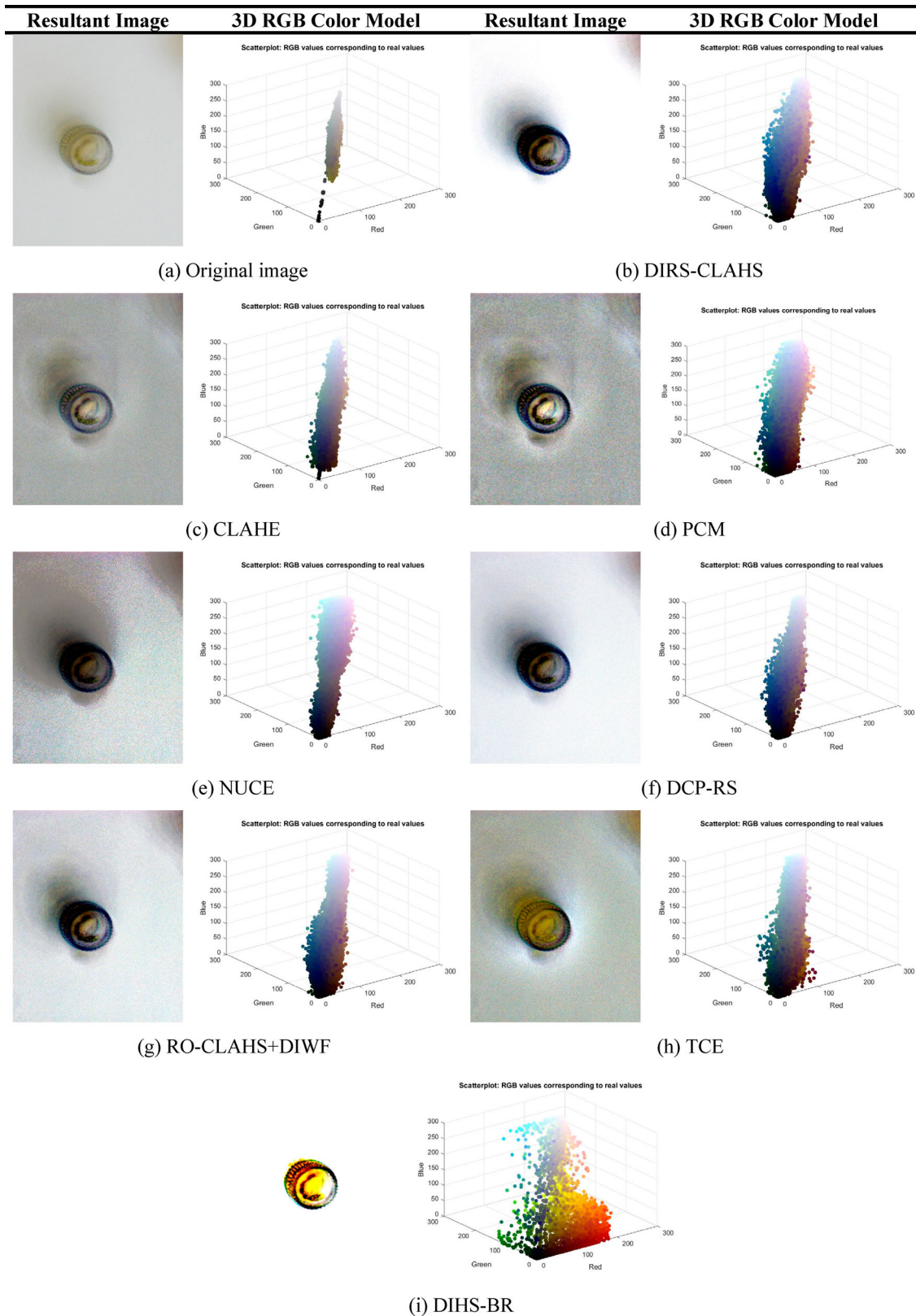


Figure 18. Image of *Cyclotella*: (a) original image and the output images of (b) DIRS-CLAHS, (c) CLAHE, (d) PCM, (e) NUCE, (f) DCP-RS, (g) RO-CLAHS + DIWF, (h) TCE, and (i) the proposed DIHS-BR method.

significantly increases the edge contrast of the phytoplankton cell.

Cyclotella and *Cocconeis* in Figures 18 and 19 show that the resultant images produced by DIRS-CLAHS (Figure 18(b) and Figure 19(b)) demonstrated improved overall appearance when the noise and haze are

minimized. The background of the images is significantly improved because all debris and floating particles are removed. However, the images are under-contrast because the phytoplankton cell areas seem dark and difficult to identify. Similar effects have been observed to the output images of the NUCE, DCP-RS, and RO-

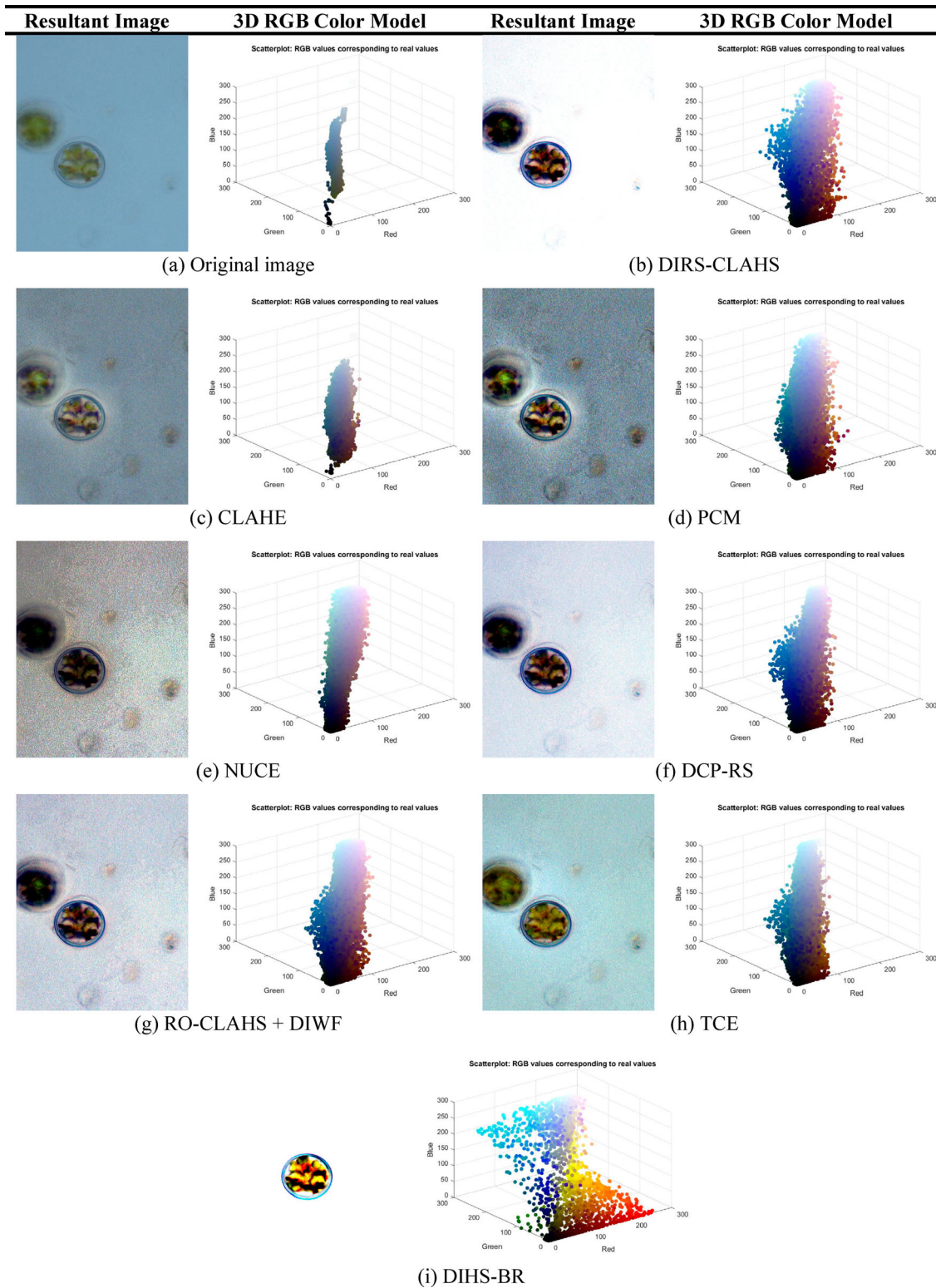


Figure 19. Image of *Cocconeis*: (a) original image and the output images of (b) DIRS-CLAHS, (c) CLAHE, (d) PCM, (e) NUCE, (f) DCP-RS, (g) RO-CLAHS + DIWF, (h) TCE, and (i) the proposed DIHS-BR method.

CLAHS + DIWF methods (Figures 18e–g) because the phytoplankton cells are considerably dark due to under-contrast. Furthermore, these methods reduce the image colour, resulting in low saturation and brightness.

CLAHE and PCM (Figures 18c and d) enhance the image contrast and produce sharp edge cells. However, the image background produces a large amount of noise because it transforms the image

phase into magnitude variations to improve the image structural details and visibility. TCE (Figure 18h) produces a low-quality image because the image output is under-contrast, and the surrounding areas seem dark. Furthermore, this method has more blurred edges of the phytoplankton cells in the image even after implementing a Gaussian filter to reduce the image noise level.

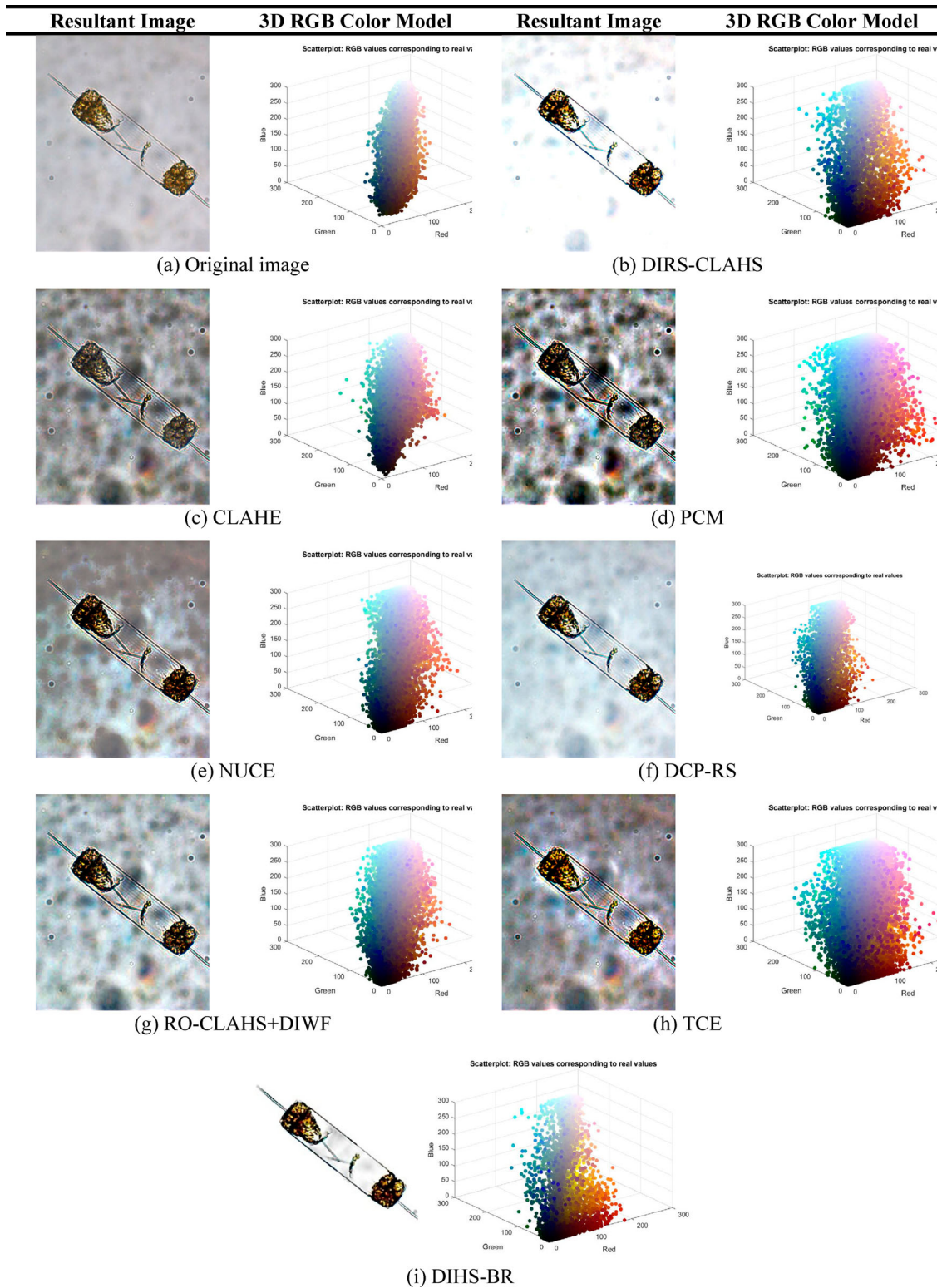


Figure 20. Image of *Hemialus*: (a) original image and the output images of (b) DIRS-CLAHS, (c) CLAHE, (d) PCM, (e) NUCE, (f) DCP-RS, (g) RO-CLAHS + DIWF, (h) TCE, and (i) the proposed DIHS-BR method.

The DIHS-BR method (Figure 18i) produces the best output result in terms of contrast, colour, and brightness. This method enhances the overall image and removes the image background in the final output, leaving only the phytoplankton cell. The image shows that the cell edge contrast is sharp after removing the noises by applying the haze removal technique. Furthermore, the contrast and brightness are

highly improved. Based on the visual observation, no over – or under-enhanced areas are visible in the output image. The quantitative evaluation supports the reason because this method produces the highest EBCM with a value of 82.621.

With regard to the *Hemialus* image in Figures 20(b) and (f), DIRS-CLAHS and DCP-RS improved the image contrast and eliminated noise. However, the image's

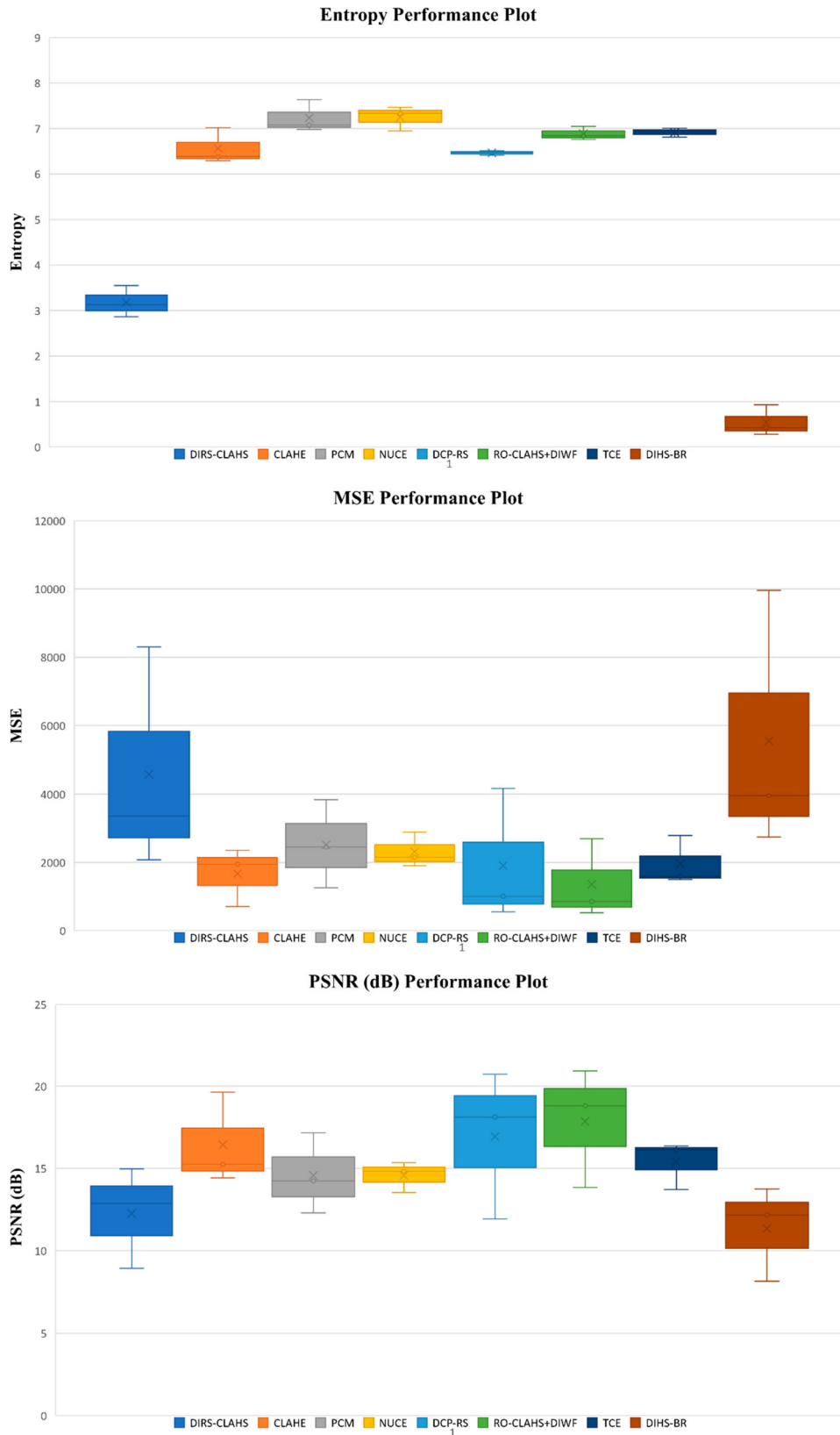


Figure 21. Distribution of the average performance evaluation in terms of entropy, MSE, PSNR, AMBE, UIQI, and EBCM.

background still contains a dark spot and makes the phytoplankton cell difficult to observe. Meanwhile, PCM (Figure 20d) produces a low-quality output image with noises due to the over-contrast, resulting in a darkened phytoplankton cell. CLAHE and TCE under-enhance the overall appearance of the output images. RO-CLAHS +

DIWF (Figure 20g) increases the cell's brightness and colour, but it produces a large amount of noise in the background. The phytoplankton cell is still difficult to observe because the background colour is dark. DIHS-BR is the best method for enhancing the overall phytoplankton cell in terms of contrast, edge, brightness,

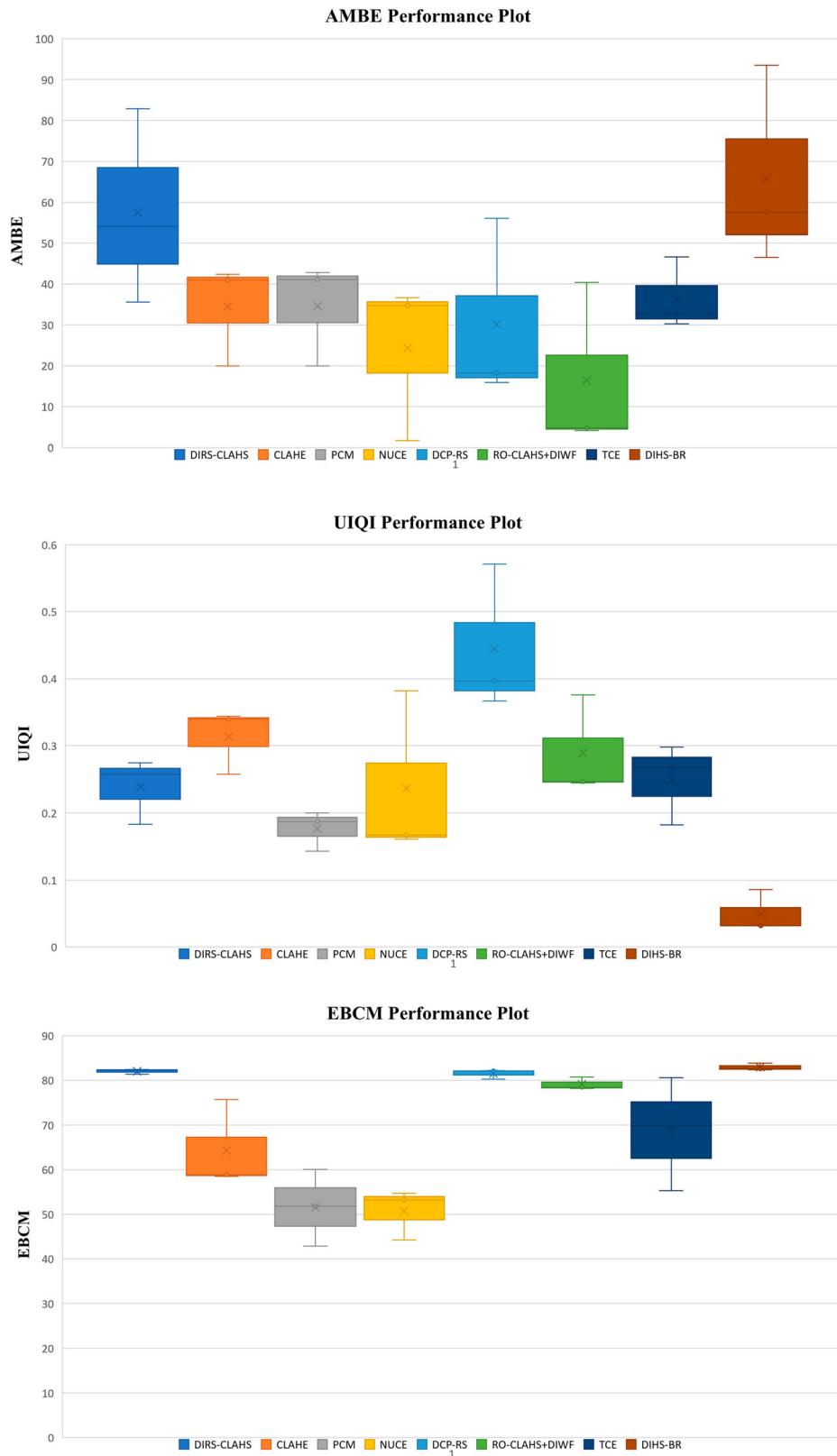


Figure 21. *Continued*

details, and noise reduction. Quantitative evaluation shows that the DIHS-BR method produces the highest values of EBCM for images in Figures 18–20 with values of 82.621, 83.828, and 82.364, respectively.

Figure 21 represents the distribution of the respective quantitative performance range of the compared methods in terms of entropy, MSE, PSNR, AMBE, UIQI,

and EBCM. Not all quantitative evaluations show significant results because the main and best evaluation of the proposed DIHS-BR method is by qualitative evaluation through the HVS. Furthermore, the objective of the proposed method is to successfully extract the phytoplankton cell for the identification and classification processes.

Table 2. Average performance of the enhancement techniques for Figures 18–20.

Method	Qualitative performance measures						Processing time (s)
	Entropy ↑	MSE ↓	PSNR ↑	AMBE ↓	UIQI ↑	EBCM ↑	
DIRS-CLAHS	3.180	4579	12.257	57.518	0.239	82.022	1.368
CLAHE	6.564	1668	16.430	34.465	0.314	64.350	0.588
PCM	7.230	2512	14.560	34.636	0.177	51.569	2.093
NUCE	7.244	2312	14.557	24.362	0.237	50.724	48.454
DGP-RS	6.462	1906	16.925	30.061	0.445	81.462	0.834
RO-CLAHS + DIWF	6.882	1358	17.853	16.467	0.289	79.097	1.065
TCE	6.912	1962	15.392	36.512	0.249	68.556	0.810
DIHS-BR	0.546	5554	11.350	65.864	0.050	82.938	1.545

Note: The value in bold represents the best result from the comparison.

Table 3. Average dataset performance of the proposed DIHS-BR method for 100 samples of phytoplankton images.

Method	Qualitative performance measures						Processing time (s)
	Entropy ↑	MSE ↓	PSNR ↑	AMBE ↓	UIQI ↑	EBCM ↑	
DIRS-CLAHS	4.170	13371	8.102	99.178	0.215	80.715	1.598
CLAHE	6.525	994	18.920	23.722	0.384	31.425	0.906
PCM	7.160	2108	15.720	25.057	0.210	35.363	2.562
NUCE	7.071	3385	14.178	38.764	0.265	50.245	72.998
DGP-RS	6.634	5717	12.583	57.984	0.396	57.066	1.847
RO-CLAHS + DIWF	7.029	4952	12.764	51.566	0.268	55.167	1.129
TCE	6.726	4148	15.236	43.512	0.336	61.651	1.327
DIHS-BR	0.663	16193	7.094	112.121	0.049	83.065	2.173

Note: The value in bold represents the best result from the comparison.

Table 2 shows the average dataset of the quantitative evaluation for Figures 18–20 of the phytoplankton images. As previously discussed, quantitative measurement is used for the comparison and does not reflect the actual quality and the main objective of the proposed method because the proposed DIHS-BR method extracts all the background areas and retains the phytoplankton cell in the final output image. Therefore, all details of the image, except the phytoplankton cell, will be lost. The results show that the proposed DIHS-BR method produces the highest value of EBCM, indicating the significant EBCM.

Table 3 shows the average dataset of the quantitative evaluation for 100 phytoplankton images. The results demonstrate that the proposed method produces the highest value of EBCM, indicating a significant EBCM compared with the other state-of-the-art methods. Furthermore, the proposed method produces the best results in terms of contrast, edge sharpness, colour, and brightness because the phytoplankton cell is significantly removed from the background. As previously mentioned, the proposed DIHS-BR method is proposed to automatically remove the background and noise of the phytoplankton image and improves the image quality while cropping an individual image of a phytoplankton cell. Therefore, visual observation (qualitative evaluation) emphasizes the overall image quality in terms of image processing and used as the main evaluation method. In this work, quantitative measurements are to support qualitative impressions. However, since the main purpose of this research work is to extract the phytoplankton cell while removing the background and other foreign particles which are parts of the original image, the proposed method

is reducing the quantitative image details (measured through entropy and universal image quality index (UIQI)) as the image background except the phytoplankton cell are removed. Meanwhile, the mean squared error (MSE) will increase and the peak signal-to-noise ratio (PSNR) will decrease because the extracted output image is different from the input image due to the removal of the output image's background. The primary comparative measurement to prove the effectiveness of the proposed DIHS-BR method is still the qualitative evaluation. The quantitative evaluation in Table 3 is for the purpose of comparison with other methods and for experimental purposes if the quantitative measurements agree with qualitative evaluations.

Using MATLAB R2021a which is installed on a Microsoft Windows 10 with Intel Core i5, 2.90 GHz, 8BG RAM, the average processing time to run the whole algorithm for a single image with size of 1280×1024 pixels is around 2 s. The overall processing time of 2 s is deemed low and comparable with other state-of-the-art methods for the best extraction results of the phytoplankton cell. Experimental results show that the proposed algorithm is suitable for practical uses as the resultant images are in considerable quality and the phytoplankton cell are highly visible and separated from the background. The Appendix contains more sample images of the extracted phytoplankton cells.

In the proposed DIHS-BR method, only the required phytoplankton cell image should appear in the final output image for cell identification and classification. Both qualitative and quantitative evaluations are used to evaluate the final results. However, qualitative evaluation is used as the main evaluation method, as

the main purpose of the research work is to extract the phytoplankton cell from the background. Removing all unwanted background results in large differences between the output image and the original image, as most quantitative measurements do. Quantitative measurements should support the qualitative evaluation. In addition, the result of the proposed method is also compared to the other state-of-the-art methods as described in Section 4.

Conclusion

The proposed DIHS-BR method consists of two major steps. The first major step is contrast adaptive histogram specification by means of dual intensity images and involves modified global contrast correction, enhanced local contrast correction, and colour correction. On the other hand, the second step refers to enhanced background removal which is designed improved mask cropping and haze removal.

The experimental results shown that the proposed DIHS-BR method has successfully extract the individual phytoplankton cell while enhancing the overall image of phytoplankton cells in terms of contrast, colour, details, brightness, edge sharpness, and noise elimination as compared with the other state-of-the-art methods. The results show that the proposed DIHS-BR method significantly improves the visibility and details of the object in an image. DIHS-BR method is proposed as a pre-processing step for the preparation toward phytoplankton detection and classification.

Nevertheless, in some cases, when more than one type of phytoplankton exists in an image, the proposed method tends to extract only the complete shape of the phytoplankton or it could extract all of these phytoplankton if these phytoplankton are located and touching side by side to each other or overlapped to each other. Otherwise, the proposed algorithm will consider these as background. This limitation will be considered as the future work of this research.

Data Availability Statement

Some data are confidential including the code. Some data are made available upon request after the publication.

Acknowledgements

The authors would like to thank all reviewers for their encouraging comments in improving this work.

Disclosure statement

We would like to declare that we do not have any commercial or associative interest that represents a conflict of interest with the work submitted.

Funding

This research has been supported by the collaborative work of the Universiti Malaysia Pahang (UMP), International Islamic University Malaysia (IIUM), and Universiti Teknologi MARA (UiTM) under University Research Grant (RDU200745) entitled 'Formulation of Mathematical Model to Enhance Underwater Image Quality Using Optimized Dehazing Method for Fluid-Type Algae Identification' and research grant of the Universiti Malaysia Pahang Postgraduate Research Scheme (PGRS210363).

Notes on contributors

Mohd Aiman Syahmi Kamarul Baharin received B.Eng. degree in Mechatronics from Universiti Malaysia Pahang (UMP), Malaysia in 2021. Currently he is pursuing his Master degree at the Faculty of Manufacturing and Mechatronic Engineering Technology in image processing and computer vision. His research interests include image enhancement, object identification, detection, classification, and machine learning.

Ahmad Shahrizan Abdul Ghani received his Master degree in Mechatronics Engineering from University of Applied Sciences Augsburg, Germany in 2009. In 2015, he obtained his PhD. Degree from Universiti Sains Malaysia (USM) in the areas of image processing and computer vision. He is currently a member of Malaysian Board of Engineer as well as Malaysian Board of Technologist. Since 2016, he is actively participated in teaching and research activities in Mechatronics and Image Processing areas. He has published various research papers on top journals and conferences, reviews journal and conference papers, and involves in various international conference. He is actively engaged and collaborates with industries. His research interests include computer vision, image processing, machine learning, and their applications.

Normawaty Mohammad Noor, PhD, is an Associate Professor of the Department of Marine Science, Kulliyah of Science, International Islamic University Malaysia (IIUM), Malaysia. Her PhD was on Marine Biology from University of Copenhagen, Denmark. Her main research interest is on taxonomy and ecology of marine algae. She has been working on this field for more than 15 years. She has published numerous scientific publications and books.

Hasnun Nita Ismail, PhD is a Senior Lecturer of Faculty of Science, University Technology MARA of Perak Branch Tapah Campus, Malaysia. Her research area focuses on water quality analysis and plankton ecology (phytoplankton and zooplankton) since the year of 2000. She has published her research findings in several book chapters, journal articles, and articles for scientific magazines at national and international levels. Presently, she has expanded her research interest to the biological study on the freshwater apple snail as a pest species in the rice field.

Syafiq Qhushairy Syamsul Amri received the B.Eng. degree in Mechatronics from Universiti Malaysia Pahang (UMP), Malaysia in 2021. He is a Master candidate at the Faculty of Manufacturing and Mechatronics Engineering Technology in the areas of image processing and computer vision. His current research interest includes underwater image enhancement, robotics, and deep learning. He is also actively participated in industrial attachment with a robotics company.

ORCID

Ahmad Shahrizan Abdul Ghani  <http://orcid.org/0000-0003-0442-7629>

References

- [1] De Tommasi E, Gielis J, Rogato A. Diatom frustule morphogenesis and function: a multidisciplinary survey. *Mar. Genomics.* 2017;35(July):1–18. doi:10.1016/j.margen.2017.07.001.
- [2] Luo Q, Gao Y, Luo J, et al. Automatic identification of diatoms with circular shape using texture analysis. *J. Softw.* 2011;6(3):428–435. doi:10.4304/jsw.6.3.428-435.
- [3] Santhi N, Pradeepa C, Subashini P, et al. Automatic identification of algal community from microscopic images. *Bioinform. Biol. Insights.* 2013;7:327–334. doi:10.4137/BBI.S12844.
- [4] Borges VRP, Oliveira MCFD, Silva TG, et al. Region growing for segmenting green microalgae images. *IEEE/ACM Trans. Comput. Biol. Bioinforma.* 2018;15(1):257–270. doi:10.1109/TCBB.2016.2615606.
- [5] Biswas B, Roy P, Choudhuri R, et al. Microscopic image contrast and brightness enhancement using multi-scale retinex and cuckoo search algorithm. *Procedia Comput. Sci.* 2015;70:348–354. doi:10.1016/j.procs.2015.10.031.
- [6] Mosleh MAA, Manssor H, Malek S, et al. A preliminary study on automated freshwater algae recognition and classification system. *BMC Bioinformatics* 2012;13 (Suppl 17). doi:10.1186/1471-2105-13-s17-s25
- [7] Somasekar J, Reddy BE. Contrast-enhanced microscopic imaging of Malaria parasites. 2014 IEEE Int. Conf. Comput. Intell. Comput. Res. IEEE ICCIC 2014, no. c, pp. 0–3, 2015. doi:10.1109/ICCIC.2014.7238439
- [8] Albán E, Leveelahti L, Heiskanen KM, et al. Color enhancement and edge detection for confocal microscopy fluorescent images. *Rep. - Helsinki Univ. Technol. Signal Process. Lab.* 2004;46(April):9–12. doi:10.1109/NORSIG.2004.250113.
- [9] Cheng J, Ji G, Feng C, et al. Application of connected morphological operators to image smoothing and edge detection of algae. *Proc. - 2009 Int. Conf. Inf. Technol. Comput. Sci. ITCS 2009*, vol. 2, pp. 73–76, 2009. doi:10.1109/ITCS.2009.153
- [10] Chen W, Mao X, Ma H. Low-contrast microscopic image enhancement based on multi-technology fusion. 2010 IEEE International Conference on Intelligent Computing and Intelligent Systems; 2010. p. 891–895. DOI:10.1109/ICICISYS.2010.5658369
- [11] Ooi CH, Kong NSP, Ibrahim H, et al. Enhancement of color microscopic images using toboggan method. *Proc. - 2009 Int. Conf. Futur. Comput. Commun. ICFCC 2009*, pp. 203–205, 2009. doi:10.1109/ICFCC.2009.81
- [12] Abdul Ghani AS, Mat Isa NA. Enhancement of low quality underwater image through integrated global and local contrast correction. *Appl. Soft Comput. J.* 2015;37:332–344. doi:10.1016/j.asoc.2015.08.033.
- [13] Cakir S, Kahraman DC, Cetin-Atalay R, et al. Contrast enhancement of microscopy images using image phase information. *IEEE Access.* 2018;6(April):3839–3850. doi:10.1109/ACCESS.2018.2796646.
- [14] Abdul Ghani AS. Image contrast enhancement using an integration of recursive-overlapped contrast limited adaptive histogram specification and dual-image wavelet fusion for the high visibility of deep underwater image. *Ocean Eng.* 2018;162:224–238. doi:10.1016/j.oceaneng.2018.05.027.
- [15] Sonali, S. Sahu, A. K. Singh, et al. “An approach for de-noising and contrast enhancement of retinal fundus image using CLAHE,” *Opt. Laser Technol.*, vol. 110, pp. 87–98, 2019, doi:10.1016/j.optlastec.2018.06.061.
- [16] Stephen KEM, Pizer M, Eugene Johnston R, et al. Contrast-limited adaptive histogram equalization: speed and effectiveness. *IEEE.* 1990;148:148–162.
- [17] Mohd Azmi KZ, Abdul Ghani AS, Md Yusof Z, et al. Natural-based underwater image color enhancement through fusion of swarm-intelligence algorithm. *Appl. Soft Comput. J.* 2019;85:105810. doi:10.1016/j.asoc.2019.105810.
- [18] Jackson J, Kun S, Agyekum KO, et al. A fast single-image dehazing algorithm based on dark channel prior and Rayleigh scattering. *IEEE Access.* 2020;8(2):73330–73339. doi:10.1109/ACCESS.2020.2988144.
- [19] Muniraj M, Dhandapani V. Underwater image enhancement by combining color constancy and dehazing based on depth estimation. *Neurocomputing.* 2021;460:211–230. doi:10.1016/j.neucom.2021.07.003.
- [20] Liu X, Gao Z, Chen BM. IPMGAN: integrating physical model and generative adversarial network for underwater image enhancement. *Neurocomputing.* 2021;453:538–551. doi:10.1016/j.neucom.2020.07.130.
- [21] Hosseini-Fard E, Roshandel-Kahoo A, Soleimani-Monfared M, et al. Automatic seismic image segmentation by introducing a novel strategy in histogram of oriented gradients. *J. Pet. Sci. Eng.* 2022;209 (October 2021):109971, doi:10.1016/j.petrol.2021.109971.
- [22] Li C, Guo C, Guo J, et al. PDR-Net: perception-inspired single image dehazing network with refinement. *IEEE Trans. Multimed.* 2020;22(3):704–716. doi:10.1109/TMM.2019.2933334.
- [23] Yang X, Li H, Fan YL, et al. Single image haze removal via region detection network. *IEEE Trans. Multimed.* 2019;21(10):2545–2560. doi:10.1109/TMM.2019.2908375.
- [24] Tom F, Sharma H, Mundhra D, et al. Learning a deep convolution network with turing test adversaries for microscopy image super resolution. *Proc. - Int. Symp. Biomed. Imaging*, vol. 2019-April, no. Isbi, pp. 1391–1394, 2019. doi:10.1109/ISBI.2019.8759443
- [25] Mohammad-Noor N, Rahaida Harun SN, Lazim ZM, et al. Diversity of phytoplankton in coastal water of Kuantan, Pahang, Malaysia. *Malaysian J. Sci.* 2013;32(1):29–37. doi:10.22452/mjs.vol32no1.6.
- [26] McGaraghan A. *Phytoplankton Identification. A guide to the marine and freshwater phytoplankton of California*, 2018.
- [27] Science C, Engineering E. Fast efficient algorithm for enhancement of low lighting video Xuan Dong, Guan Wang *, Yi (Amy) Pang, Weixin Li *, Jiangtao (Gene) Wen, Wei Meng, Yao Lu **. *Differences.* 2011;3:3–8.
- [28] Zhang L, Wang X, She C. Single image haze removal based on saliency detection and dark channel prior. *Proc. - Int. Conf. Image Process. ICIP*, vol. 2017-Septe, pp. 4292–4296, 2018. doi:10.1109/ICIP.2017.8297092
- [29] Shashev D. Image processing in intelligent medical robotic systems. *MATEC Web Conf.* 79, 01050, 2016. doi:10.1108/aa.1998.03318cad.010

- [30] Gonzalez RC, Woods RE, Eddins SL. Digital image processing using MATLAB. United States of America: Gatesmark Publishing; 2009.
- [31] Adams R. Radial decomposition of disks and spheres. *Comput.: Vision, Graph. Image Process. Graph. Model. Image Process.* 1993;55(5):325–332.
- [32] Ghani ASA, Aris RSNAR, Zain MLM. Unsupervised contrast correction for underwater image quality enhancement through integrated-intensity stretched-Rayleigh histograms. *J. Telecommun. Electron. Comput. Eng.* 2016;8(3):1–7.
- [33] Harun NH, Bakar JA, Wahab ZA, et al. Color image enhancement of acute leukemia cells in blood microscopic image for leukemia detection sample. ISCAIE 2020 - IEEE 10th Symp. Comput. Appl. Ind. Electron, no. 3, pp. 24–29, 2020. doi:10.1109/ISCAIE47305.2020.9108810
- [34] Gupta B, Tiwari M. Minimum mean brightness error contrast enhancement of color images using adaptive gamma correction with color preserving framework. *Optik (Stuttg).* 2016;127(4):1671–1676. doi:10.1016/j.ijleo.2015.10.068.
- [35] Wang Z, Bovik AC. A universal image quality index. *IEEE Signal Process. Lett.* 2002;9(3):81–84. doi:10.1109/97.995823.
- [36] Beghdadi A, Le Negrate A. Contrast enhancement technique based on local detection of edges. *Comput. Vision, Graph. Image Process.* 1989;46(2):162–174. doi:10.1016/0734-189X(89)90166-7.

Appendices

Appendix A

Original image	DIRS-CLAHS	CLAHE	PCM	NUCE	DCP-RS	RO-CLAHS + DIWF	TCE	DIHS-BR
Image 1								
Image 2								
Image 3								
Image 4								
Image 5								
Image 6								
Image 7								

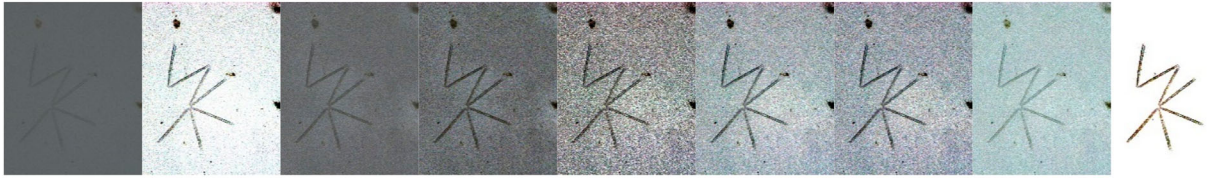


Image 8

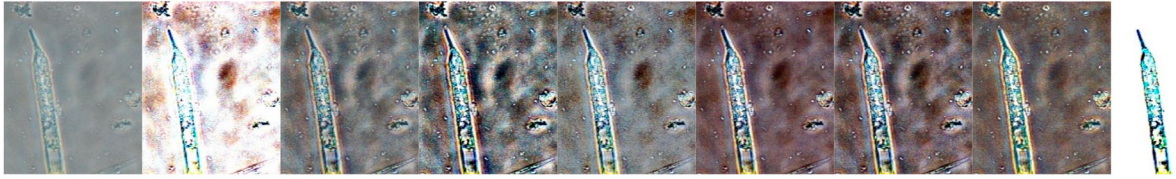


Image 9

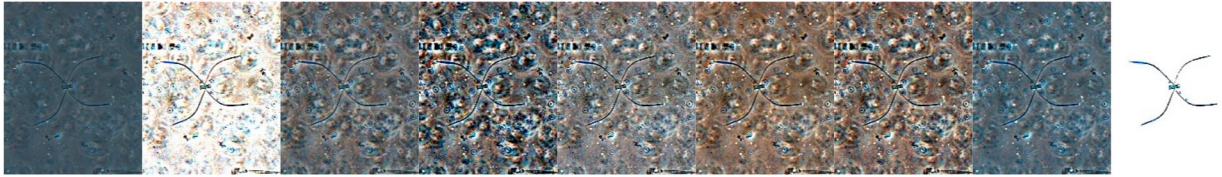


Image 10



Image 11



Image 12

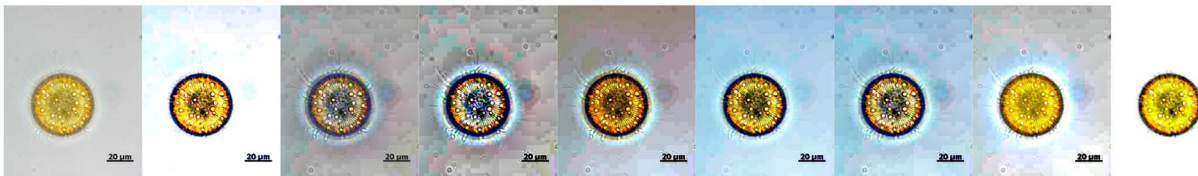


Image 13

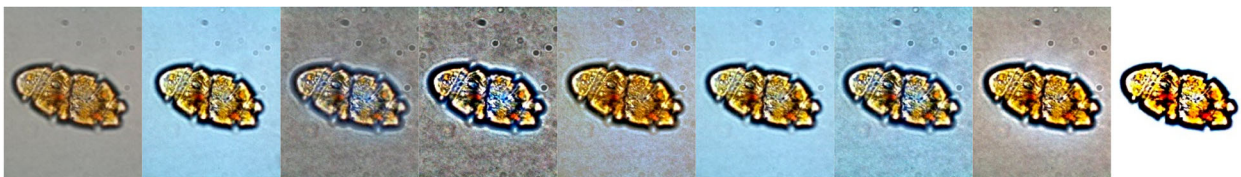


Image 14

Appendix B

Quantitative evaluations of the images in Appendix A.

Figure	Method	Qualitative performance measures					
		Entropy ↑	MSE ↓	PSNR ↑	AMBE ↓	UIQI ↑	EBCM ↑
Image 1	DIRS-CLAHS	5.4171	23184.800	4.4788	145.477	0.205	81.012
	CLAHE	6.720	859.022	18.791	23.314	0.424	16.567
	PCM	7.447	2129.396	14.848	23.451	0.230	28.978
	NUCE	6.795	2877.541	13.541	47.143	0.303	44.814
	DGP-RS	6.700	1345.469	16.842	28.618	0.455	29.089
	RO-CLAHS + DIWF	7.127	1775.264	15.638	30.188	0.314	33.518
	TCE	6.381	682.944	19.787	18.321	0.502	9.954
	DIHS-BR	0.422	29050.444	3.500	165.350	0.039	83.681
Image 2	DIRS-CLAHS	2.928	24917.764	4.166	152.246	0.216	82.525
	CLAHE	5.988	472.924	21.383	17.765	0.401	9.115
	PCM	6.830	925.001	18.469	18.088	0.222	23.351
	NUCE	7.352	6425.441	10.052	64.834	0.118	40.792
	DGP-RS	5.966	18694.507	5.414	131.415	0.261	82.005
	RO-CLAHS + DIWF	6.531	14850.921	6.413	116.040	0.184	81.203
	TCE	6.409	12533.215	7.150	106.540	0.218	81.885
	DIHS-BR	0.390	26915.425	3.831	159.497	0.033	84.197
Image 3	DIRS-CLAHS	4.579	2834.951	13.605	36.360	0.289	77.618
	CLAHE	6.690	1858.456	15.439	38.038	0.362	64.687
	PCM	7.330	3810.731	12.321	46.298	0.212	47.397
	NUCE	6.563	3547.226	12.632	53.238	0.410	49.977
	DGP-RS	6.682	3608.450	12.558	50.884	0.493	44.737
	RO-CLAHS + DIWF	6.862	4111.205	11.991	56.014	0.330	37.154
	TCE	7.100	2781.417	13.688	42.509	0.337	63.312
	DIHS-BR	0.460	4463.855	11.634	58.031	0.082	84.219
Image 4	DIRS-CLAHS	5.558	6713.025	9.862	73.802	0.302	79.511
	CLAHE	7.433	1413.705	16.627	24.018	0.441	36.030
	PCM	7.644	4062.110	12.043	24.637	0.232	37.870
	NUCE	7.243	804.860	19.074	14.300	0.423	44.914
	DGP-RS	7.235	1221.540	17.262	23.423	0.564	26.587
	RO-CLAHS + DIWF	7.626	2062.353	14.987	26.532	0.368	34.051
	TCE	7.179	1238.164	17.203	18.777	0.423	35.499
	DIHS-BR	0.918	11000.267	7.717	97.038	0.045	82.839
Image 5	DIRS-CLAHS	5.314	21992.215	4.708	140.973	0.112	80.697
	CLAHE	5.672	349.919	22.691	15.639	0.353	4.876
	PCM	6.614	698.616	19.688	15.640	0.192	23.041
	NUCE	7.582	6497.675	10.003	57.986	0.080	46.088
	DGP-RS	7.135	9806.926	8.216	89.762	0.110	55.603
	RO-CLAHS + DIWF	7.301	8365.614	8.906	80.351	0.102	44.242
	TCE	6.610	10642.060	7.861	98.420	0.152	80.746
	DIHS-BR	6.310	4625.516	11.479	61.394	0.056	82.779
Image 6	DIRS-CLAHS	3.149	4657.029	11.450	55.366	0.227	82.898
	CLAHE	6.722	1507.890	16.347	33.566	1.304	43.799
	PCM	7.174	1978.515	15.167	33.510	0.166	44.664
	NUCE	7.125	2972.587	13.400	20.720	0.155	46.817
	DGP-RS	5.785	2339.825	14.439	37.625	0.324	82.567
	RO-CLAHS + DIWF	6.574	1640.706	15.981	21.229	0.212	82.074
	TCE	6.665	591.693	20.410	11.467	0.344	82.881
	DIHS-BR	0.465	5381.522	10.822	59.690	0.038	83.347
Image 7	DIRS-CLAHS	2.385	1552.992	16.219	9.504	0.104	78.208
	CLAHE	6.555	2496.256	14.158	45.297	0.220	76.551
	PCM	7.180	3425.613	12.783	45.557	0.120	73.790
	NUCE	7.509	4342.843	11.753	47.465	0.117	61.840
	DGP-RS	6.335	1493.350	16.389	7.387	0.263	76.523
	RO-CLAHS + DIWF	6.716	1660.462	15.929	15.498	0.191	76.078
	TCE	7.029	2249.527	14.610	27.487	0.164	77.643
	DIHS-BR	0.877	1525.283	16.297	21.731	0.048	82.376
Image 8	DIRS-CLAHS	5.446	18076.610	5.560	126.817	0.114	79.552
	CLAHE	5.667	163.739	25.990	8.519	0.357	80.172
	PCM	6.616	511.633	21.041	8.518	0.194	30.767
	NUCE	7.603	4668.048	11.440	42.604	0.087	45.856
	DGP-RS	7.184	6230.173	10.186	68.410	0.118	46.819
	RO-CLAHS + DIWF	7.335	5514.343	10.716	61.324	0.110	41.641
	TCE	6.530	9007.818	8.585	90.605	0.177	81.348
	DIHS-BR	0.423	23163.955	4.483	147.427	0.031	83.997
Image 9	DIRS-CLAHS	5.834	7064.788	9.640	72.045	0.225	79.780
	CLAHE	6.904	848.905	18.842	20.677	0.405	34.140
	PCM	7.572	2390.737	14.346	20.971	0.217	36.873
	NUCE	7.163	1167.745	17.457	16.874	0.289	43.794
	DGP-RS	7.026	3025.204	13.323	46.196	0.417	18.701
	RO-CLAHS + DIWF	7.350	2743.574	13.748	38.260	0.299	28.524
	TCE	6.808	2180.885	14.745	37.936	0.357	23.013
	DIHS-BR	0.482	11836.185	7.399	102.448	0.039	83.024

(Continued)

Continued.

Figure	Method	Qualitative performance measures					
		Entropy ↑	MSE ↓	PSNR ↑	AMBE ↓	UIQI ↑	EBCM ↑
Image 10	DIRS-CLAHS	5.717	19587.985	5.211	131.239	0.171	79.103
	CLAHE	6.948	961.763	18.300	21.357	0.404	21.684
	PCM	7.661	2807.512	13.648	21.560	0.217	30.177
	NUCE	7.297	3016.960	13.335	42.131	0.234	42.139
	DCP-RS	7.239	2185.854	14.735	29.900	0.323	40.905
	RO-CLAHS + DIWF	7.483	2584.733	14.007	30.527	0.261	37.773
	TCE	6.723	667.926	19.884	19.268	0.512	9.884
	DIHS-BR	0.174	27500.168	3.738	161.205	0.031	84.416
Image 11	DIRS-CLAHS	3.833	3949.161	12.166	58.181	0.242	83.090
	CLAHE	6.298	1460.480	16.486	35.300	0.323	69.975
	PCM	6.986	2012.853	15.093	35.360	0.194	59.674
	NUCE	6.870	1731.023	15.748	34.099	0.324	57.138
	DCP-RS	6.740	402.725	22.081	5.027	0.441	82.018
	RO-CLAHS + DIWF	6.866	525.914	20.922	8.817	0.298	77.850
	TCE	6.575	1041.560	17.954	27.179	0.297	75.525
	DIHS-BR	0.480	5231.322	10.945	68.084	0.109	83.446
Image 12	DIRS-CLAHS	3.859	2843.232	13.593	48.295	0.237	82.629
	CLAHE	6.906	2613.254	13.960	46.315	0.279	58.841
	PCM	7.540	3847.694	12.279	46.810	0.153	49.045
	NUCE	6.962	2429.894	14.275	42.752	0.276	54.410
	DCP-RS	6.794	346.413	22.735	0.961	0.430	80.923
	RO-CLAHS + DIWF	7.102	991.706	18.167	20.630	0.264	71.318
	TCE	7.139	1412.381	16.631	26.432	0.245	73.421
	DIHS-BR	0.756	3676.346	12.477	55.920	0.074	83.310
Image 13	DIRS-CLAHS	2.717	2377.998	14.369	40.715	0.637	82.011
	CLAHE	5.951	1586.916	16.125	36.188	0.382	79.411
	PCM	6.498	1991.615	15.139	36.159	0.197	77.487
	NUCE	6.566	2050.831	15.012	37.075	0.607	79.887
	DCP-RS	6.535	790.841	19.150	1.851	0.701	80.842
	RO-CLAHS + DIWF	6.939	777.629	19.223	6.567	0.419	79.907
	TCE	6.437	490.497	21.224	3.706	0.478	82.881
	DIHS-BR	1.002	2707.039	13.806	44.522	0.651	83.190
Image 14	DIRS-CLAHS	2.246	9299.564	8.446	90.022	0.157	80.745
	CLAHE	6.453	497.411	21.164	13.715	0.403	44.902
	PCM	7.084	1156.436	17.500	13.766	0.220	42.242
	NUCE	6.837	573.423	20.546	13.128	0.364	78.315
	DCP-RS	6.937	3006.656	13.350	44.160	0.570	78.575
	RO-CLAHS + DIWF	7.180	1861.009	15.433	30.605	0.364	73.925
	TCE	6.735	572.519	20.553	8.550	0.378	77.280
	DIHS-BR	1.337	9516.966	8.346	85.431	0.070	79.068

Note: The value in bold represents the best result from the comparison.